UNIVERSITY OF STELLENBOSCH

Department of Applied Mathematics

Report to the

WATER RESEARCH COMMISSION

on

MODELLING OF FLOW PHENOMENA IN POROUS MEDIA

by

J P du Plessis

WRC Report No. 585/1/95
ISBN 1 86845 177 1

PRETORIA
July 1995

ACKNOWLEDGEMENTS

The financing of the project by the Water Research Commission is gratefully acknowledged and so is the support by its members and especially Dr. T. Erasmus under whose supervision this project was conducted. The University of Stellenbosch is also gratefully acknowledged for provision of computing and administrative facilities. A special word of thanks is also forwarded to Ms. L.I. Roos, research assistant, for invaluable computational support and analytical inputs to the work.

Furthermore I would like to thank my colleagues in France for their friendship and unselfish cooperation with the research work.

EXECUTIVE SUMMARY

BACKGROUND

The two-year project reported on here formed a follow-up to a similar project done for the Water Research Commission during 1991/2 and which provided a stimilus for very advanced research on the mathematical prediction methods of water movement through porous structures.

Any analysis of water research activities will invariably show that a major part of such activities concerns flow through porous media. Standard filtration using sand beds and technically more advanced practices utilising membrane systems are but two examples of applied technology making use of flow through porous media. Naturally occurring phenomena such as water seepage through sandstone and other rock formations are governed by the same physical principles and the mathematical modelling is therefore similar. Run-off from precipitation, irrigation and spraying of farmlands also cause water movement through porous soils and the monitoring of concurrent pesticide concentration redistributions has become a problem of considerable importance.

Field research activities on these phenomena form an important aspect of many projects launched by the Water Research Commission. Managerial action on findings require extensive qualification and quantification of results and the better the modelling framework on which such elaboration takes place the better the chances are for any predictive judgment to be optimal under practical circumstances.

More often than not so-called 'mathematical models' consist of curve-fitting by linear regression techniques and the qualification of the result is measured against the tightness of the fit for the particular set of data. The produced 'mathematical model' is then an equation of some kind with some numerical coefficients of which the physical bearing is mostly unknown. In this project the emphasis is focussed on the physical origin of the type of curve against which the data is tested and the prime goal is therefore to use the physics involved to prescribe the curve being used. In this manner the coefficients are quite often reduced and, since the knowledge is available about the physical origin of the particular curve, the remaining coefficients are bounded by physical constraints. The experimental and/or numerical data are then only used to fine-trim these coefficients and much less experimental work is normally needed. Since physical length parameters of the particular case are explicitly used in the modelling, the problem of scaling is eliminated and laboratory-scale results apply directly to field-scale phenomena.

In this report the term *porous media* is used generically for any porous structure found in water research and results are understood to be applicable to flow through any practical

porous medium resembling one of the idealized structures of the theoretical analysis. Of particular importance is the flow through *synthetic membranes* and systems thereof where the membrane structure can be idealized as a composite material constructed of layers of different basic structures. The results offered in this report may thus be used straightforwardly in analyses of flow phenomena relating to seepage through membranes.

FULFILMENT OF CONTRACT OBJECTIVES

The prime objective of the project was to further improve the modelling framework for the deterministic mathematical analysis of flow phenomena in porous media and to demonstrate the enhancement of practical predictive capabilities in this field. The construction of the theoretical basis should, however, be done in such a manner that generalization of any aspect may be attempted logically. At initiation of the project the following specific aspects were proposed for special attention:

1. Contaminant transport and dispersion
2. Electrokinetic effects of ions on motion
3. Macroscopic Boundary Effects
4. Influence of Anisotropy of the Porous Structure
5. Membrane Morphology and pore diameter distribution
6. Numerical simulation techniques
7. Unsaturated flow

As is discussed in the full report, extensive progress was obtained in the majority of these aspects and, since all the activities involved research efforts with unkown outcome, this is gratifying. Except for the analysis on electrokinetic phenomena, progress is reported on all aspects considered. Viewed globally the project produced a sound theoretical basis for the analytical and computational quantification of seepage phenomena for foams and granular materials over the entire porosity and velocity spectra. This is of particular importance to research on the enhancement of water purification methods and the study of contaminant transport in groundwater systems.

Contract objectives were thus fulfilled and substantial advances were made in the predicting capabilities of modelling results for a variety of problems in water related research.

CONTRIBUTIONS TO THE STATE OF ART

A unified theory is presented by which the same physical and mathematical principles are used to obtain momentum and tracer transport equations for an almost unlimited range of practically possible porosity and microstructural length scales. The analytical predictive results are shown to be accurate over a porosity range varying from 5%, in case of granular sandstones, to 98% for foams. Lengths scales of experimentally verified results

vary between a few micrometers for sandstones and several millimeters in case of packed beds.

Careful analysis of computer simulation of average flow fields has provided insight into the influence of external boundary conditions applied and several suggestive remarks put forward to improve correlation of numerical results with experimental observation.

SIGNIFICANCE OF THIS REPORT

This report summarizes theoretical results which may be used during the predictive analyses of a great variety of water research problems, including microfiltration through synthetic membranes, groundwater, macrofiltration in packed beds and foams. Although aimed primarily at flow phenomena in synthetic membranes it is shown in this report that all results are directly applicable to several other water related research problems. In fact, since quantification of membrane morphology is so extremely difficult, the verification of the model results was done here through comparison to different porous flow phenomena for which the physical parameters of the microstructure were experimentally determinable.

MAJOR RESULTS

1. Novel sets of closure equations were derived for fluid flow and cross stream tracer dispersion through foams and granular media. These equations are provided in a form ready not only for further analysis, but also for almost direct implementation in large scale computer simulations of involved flow phenomena.

2. The pinching effect in low porosity groundwater seepage, caused by blocking of a percentage of the pores, was shown to be handled effectively by the model and experimental observations can now be predicted remarkably well.

3. Some progress was made in the field of tracer dispersion and a predictive equation for a transverse dispersion coefficient derived.

4. Anisotropicity in foam structures was shown to be handled effectively by a straightforward generalization of the model.

ACTIONS TO BE TAKEN

This research was done to provide a sound framework towards the prediction of flow and transfer processes in porous media. As such the action needed is further publication of

results in technical journals to reach such a wide group of researchers as possible. Especially important is the fact that the results are interdisciplinary applicable and it is hoped that in future this will lead to cross-fertilization between different research communities, thereby cutting down on duplication of costly experimental work.

RECOMMENDATIONS

Further research in this field will aid significantly in broadening the interdisciplinary knowledge base of water science. The theoretical expositions presented form a sound foundation on which scientific analysis of secondary effects of water seepage may be based, e.g. transport and dispersion of hazardous contaminants and multiphase phenomena.

Typical research fields in need of further development are the following:

1. Tracer dispersion.
   The theory developed in the course of the project has been demonstrated to accurately predict basic hydrodynamical phenomena as observed in nature and on laboratory scale. The underlying knowledge of flow fields must therefore be a reasonable approximation of real life situations and may therefore be used for analysis of tracer transport which may accompany water seepage in aquifers, membrane systems, filtration plants, etc.

2. Prediction of groundwater seepage.
   A novel methodology to predict pinching effects in sandstone formations was developed and shown to be effective in modelling flow disparities in very low porosity sandstones. This seemingly successful method should be investigated further with regard to comparison with more experimental evidence and other microstructures.

3. Electrokinetic effects in porous media.
   This is one aspect in which the project failed to show the anticipated progress and it is believed that, given the progress demonstrated on the other fundamental issues, the way is now paved to put analysis on elecktrokinetica phenomena on the same sound footing.

CONCLUSIONS

The extremely satisfactory prediction by the same basic theory of experimental results for vastly different physical phenomena provides confidence in the method and proves the success of the research effort over the last four years.

Contents

1 NOMENCLATURE 8

2 INTRODUCTION 11

3 BACKGROUND 13
- 3.1 Physical Problem Statement . . . 13
- 3.2 Mathematical Framework . . . 14

4 RESEARCH RESULTS 18
- 4.1 Contaminant transport and dispersion . . . 18
  - 4.1.1 Tortuosity . . . 18
  - 4.1.2 Tracer Dispersion . . . 19
- 4.2 Electrokinetic effects of ions on motion . . . 22
- 4.3 Influence of structure and pore diameter distribution . . . 22
  - 4.3.1 Foam Structures . . . 22
  - 4.3.2 Granular Structures . . . 23
- 4.4 Influence of porous structure anisotropy . . . 25
- 4.5 Numerical simulation techniques . . . 26
- 4.6 Macroscopic Boundary Effects . . . 27
  - 4.6.1 Spatial variation in porosity . . . 27
  - 4.6.2 The Ergun equation . . . 30
  - 4.6.3 Solution Method I: Control-volume discretization method . . . 31
  - 4.6.4 Solution Method II: Variational method . . . 34
  - 4.6.5 Numerical results . . . 41
  - 4.6.6 Experimental correlation . . . 42
- 4.7 Unsaturated flow . . . 44
  - 4.7.1 Massilon sandstone . . . 44
  - 4.7.2 Berea sandstone . . . 45
  - 4.7.3 Fontainebleau sandstone . . . 45

5 RESEARCH OUTPUT 48

6 PROJECT ASSESSMENT 49
- 6.1 Fulfilment of Contract Objectives . . . 49
- 6.2 Contributions to the State of Art . . . 49
- 6.3 Significance of this Report . . . 50
- 6.4 Recommendations . . . 50

7 REFERENCES 52

1 NOMENCLATURE

Alphabetic Symbols

A	integration function,
A_p	streamwise cross-sectional single pore area,
a	discretization coefficients,
a_L	longitudinal dispersivity,
a_T	transverse dispersivity,
B	integration function,
b	distance between parallel plates,
C	integration function,
c_d	interstitial form drag coefficient,
D	solid particle diameter,
$\underline{\underline{D}}$	dispersion tensor,
D_B	bed diameter,
D_L	longitudinal dispersion coefficient, $a_L q$,
D_T	transverse dispersion coefficient, $a_T q$,
d	microscopic characteristic length,
d_g	grain size,
d_p	pore width,
d_s	cube side width,
E	integral to be minimized,
E	as subscript, eastern grid point neighbour,
e	as subscript, eastern boundary of control volume,
F	microscopic shear factor,
f_1, f_2	functions of porosity ϵ,
$\boldsymbol{g}$	gravitational body force per unit mass,
H	Euler function,
h	width of parallel plates,
I	Euler function,
L_{REV}	REV scale length,
$\boldsymbol{i}$	unit vector in x-direction,
K	Darcy hydrodynamic permeability,
K	integration function,
k	constant term in discretization equation,
l	length of parallel plates / tube,
N	discretized minimization integral,
n	number of nodes in discretization grid,
P	grid point of concern,
p	intrinsic phase averaged fluid pressure,
p_i	interstitial fluid pressure,
$\overset{\circ}{p}$	pointwise pressure deviation, $p - p_f$,

Q	volume flow rate,
$\boldsymbol{q}$	phase average velocity,
q	magnitude of $\boldsymbol{q}$,
R	tube radius,
Re_{qD}	Reynolds number, $\rho\|\boldsymbol{q}\|D/\mu$,
Re_{qd}	Reynolds number, $\rho\|\boldsymbol{q}\|d/\mu$,
Re_{qs}	particle Reynolds number, $\rho q d_s/\mu$,
Re_p	sphere Reynolds number, $\rho q d_p/\mu$,
r	radial coordinate,
S	surface area,
S	source term,
$\bar{S}$	average of source term over control volume,
S_{fs}	fluid-solid interface in RUC,
t	time,
V_f	fluid filled volume within RUC,
V_o	total volume of RUC,
V_s	solid volume within RUC,
$\boldsymbol{v}$	fluid velocity field within V_f,
v_p	mean velocity in streamwise pore section,
v_t	mean velocity in transverse pore section,
W	as subscript, western grid point neighbour,
w	$q(r)\,r$,
w	as subscript, western boundary of control volume,
x	x-coordinate,
y	distance from container wall,
z	flow direction coordinate,

Greek Letters

γ	velocity ratio, v_t/v_p,
ϵ	porosity (void fraction), V_f/V_0 ,
ϵ_b	bed porosity,
ϵ_c	cut-off porosity,
ϵ_{eff}	effective porosity,
ϵ_t	threshhold porosity,
λ	pressure gradient $\partial p/\partial z$,
μ	fluid dynamic viscosity,
$\boldsymbol{\nu}$	normal surface vector on S_{fs} pointing into V_s,
ρ	fluid mass density,
ϕ	generic variable,
Ω	volume averaged tracer concentration,
ω	tracer concentration,
$\langle\phi\rangle$	volumetric phase average of ϕ, $\frac{1}{V_0}\iiint_{V_f}\phi dV$,

$\overset{\circ}{\phi}$	deviation, $\phi - \langle\phi\rangle_f$.
χ	tortuosity,

Subscripts

c	critical point,
f	fluid phase,
fs	fluid-solid interface,

Special symbols

$\nabla^2_{\parallel}$	locally streamwise laplacian,
$\nabla^2_{\perp}$	locally transverse laplacian.

2 INTRODUCTION

The research reported in this document emanated from a project funded during 1993 and 1994 by the Water Research Commission and is entitled MODELLING OF FLOW THROUGH POROUS MEDIA. This two-year project formed a follow-up to a similar project done for the Water Research Commission during 1991/2 and which provided a stimilus for very advanced research on the mathematical prediction methods of water movement through porous structures (Du Plessis, 1993a).

Any analysis of water research activities will invariably show that a major part of such activities concerns flow through porous media. Standard filtration using sand beds and technically more advanced practices utilising membrane systems are but two examples of applied technology making use of flow through porous media. Naturally occurring phenomena such as water seepage through sandstone and other rock formations are governed by the same physical principles and the mathematical modelling is therefore similar. Run-off from precipitation, irrigation and spraying of farmlands also cause water movement through porous soils and the monitoring of concurrent pesticide concentration redistributions has become a problem of considerable importance.

Field research activities on these phenomena form an important aspect of many projects launched by the Water Research Commission. Managerial action on findings require extensive qualification and quantification of results and the better the modelling framework on which such elaboration takes place the better the chances are for any predictive judgment to be optimal under practical circumstances.

More often than not so-called 'mathematical models' consist of curve-fitting by linear regression techniques and the qualification of the result is measured against the tightness of the fit for the particular set of data. The produced 'mathematical model' is then an equation of some kind with some numerical coefficients of which the physical bearing is mostly unknown. In this project the emphasis is focussed on the physical origin of the type of curve against which the data is tested and the prime goal is therefore to use the physics involved to prescribe the curve being used. In this manner the coefficients are quite often reduced and, since the knowledge is available about the physical origin of the particular curve, the remaining coefficients are bounded by physical constraints. The experimental and/or numerical data are then only used to fine-trim these coefficients and much less experimental work is normally needed. Since physical length parameters of the particular case are explicitly used in the modelling, the problem of scaling is eliminated and laboratory-scale results apply directly to field-scale phenomena.

In this report the term *porous media* is used generically for any porous structure found in water research and results are understood to be applicable to flow through any practical

porous medium resembling one of the idealized structures of the theoretical analysis. Of particular importance is the flow through *synthetic membranes* and systems thereof where the membrane structure can be idealized as a composite material constructed of layers of different basic structures. The results offered in this report may thus be used straightforwardly in the analysis of flow phenomena relating to seepage through membranes.

OBJECTIVES

The prime goal of the project was to further improve the modelling framework for the deterministic mathematical analysis of flow phenomena in porous media and to demonstrate the enhancement of practical predictive capabilities in this field. At initiation of the project the following specific aspects were proposed for special attention:

1. Contaminant transport and dispersion
2. Electrokinetic effects of ions on motion
3. Macroscopic Boundary Effects
4. Influence of Anisotropy of the Porous Structure
5. Membrane Morphology and pore diameter distribution
6. Numerical simulation techniques
7. Unsaturated flow

As will be discussed in this report, remarkable progress was obtained in the majority of these aspects.

3 BACKGROUND

3.1 Physical Problem Statement

The physical problem analyzed consists of the special case of two-phase flow where one phase forms a porous structure and the second phase is a fluid. The set of constraints given below is used to keep the analysis simple and staightforward. The construction of the theoretical basis is, however, done in such a manner that generalization of any aspect may be attempted logically.

Solid phase properties
The porous medium under consideration is assumed to be stationary and its structure is assumed to be morphologically isotropic unless explicitly stated otherwise. The porous structure is assumed to be a composite construction of different kinds of porous domains each of which can be described by one of the four basic geometric pore-structure models proposed, namely foamlike, granular, tubular and prismatic.

Fluid Phase Properties
The traversing fluid is assumed to consist of a single phase Newtonian fluid of constant density and viscosity as is appropriate for water. It is thus also implicitly assumed here that we are dealing only with cases of fully saturated flow conditions.

Interstitial Flow Conditions
The microscopic interstitial flow conditions in the porous medium channels are considered laminar and a no-slip boundary condition on velocity is assumed unless explicitly stated otherwise.

Average Flow Conditions
The macroscopic average velocity gradients are assumed to be small as is normally the situation in phenomena related to water seepage.

3.2 Mathematical Framework

Subject to the assumptions stated above the flow through the porous structure is governed by the continuity equation,

$$\nabla \cdot \boldsymbol{v} = 0, \tag{1}$$

expressing conservation of mass, and the Navier-Stokes equation,

$$\rho \frac{\partial \boldsymbol{v}}{\partial t} + \rho \, \nabla \cdot \boldsymbol{v}\boldsymbol{v} + \nabla p_i - \rho \boldsymbol{g} - \mu \nabla^2 \boldsymbol{v} = \boldsymbol{0}, \tag{2}$$

governing the transport of momentum.

Since it is practically impossible to explicitly describe the flow in each channel section in the porous medium an averaging procedure is introduced whereby all parameters are volumetrically averaged over some control volume V_0 (Bachmat and Bear, 1986). Each fluid-related quantity or term is volumetrically averaged over the fluid part V_f of V_0 and multiplied by the porosity to yield an average over the entire volume V_0, the porosity being defined by

$$\epsilon \equiv \frac{V_f}{V_0} \tag{3}$$

The specific discharge $\boldsymbol{q}$ denotes the volume average of the fluid velocity within the pores and it will be used here as dependent variable in the averaged equations. This vectorial quantity also determines the *local streamwise direction.* It follows directly from the volumetric averaging of the actual interstitial velocity $\boldsymbol{v}$, namely

$$\boldsymbol{q} \equiv <\boldsymbol{v}> = \frac{1}{V_0} \iiint_{V_f} \boldsymbol{v} \, dV = \frac{\epsilon}{V_f} \iiint_{V_f} \boldsymbol{v} \, dV \tag{4}$$

Volumetric phase averaging (Bear and Bachmat, 1986) of the continuity equation (5) yields the following generalized equation for fluid mass conservation during its traversing of a porous medium:

$$\boldsymbol{\nabla}\cdot\boldsymbol{q} = 0. \tag{5}$$

Similarly the volumetrically averaged form of the Navier-Stokes equation (2) can be written as (Du Plessis and Masliyah, 1988):

$$\rho\frac{\partial \boldsymbol{q}}{\partial t} + \rho\,\boldsymbol{\nabla}\cdot(\boldsymbol{q}\boldsymbol{q}/\epsilon) + \epsilon\boldsymbol{\nabla}p - \epsilon\rho\boldsymbol{g} - \mu\nabla^2\boldsymbol{q} + \frac{\rho}{V_0}\iiint_{V_f}\boldsymbol{\nabla}\cdot(\mathring{\boldsymbol{v}}\mathring{\boldsymbol{v}})dV - \frac{1}{V_0}\iint_{S_{fs}}\left(-\mathring{p}\,\boldsymbol{\nu} + \mu\boldsymbol{\nu}\cdot\boldsymbol{\nabla}\boldsymbol{v}\right)dS = \boldsymbol{0}. \tag{6}$$

Due to the assumption that no large velocity gradients are present the volume integral of the velocity dispersion should be very small and the sixth term involving the volume integral may thus be discarded in comparison with the other terms present.

The evaluation of the surface integral in equation (6) is subject to a description of the real velocity gradients at the pore surfaces. This in turn warrants a fairly accurate description of the porous microstructure. The momentum transport in this form thus still remain 'open' in the sense that more information on the particular pore structure and flow conditions are needed to evaluate the surface integral and thus obtain a closed solution of practical use.

It was shown by Du Plessis and Masliyah, 1991, that pore-scale modelling of the structure may conveniently lead to the following general momentum transport equation:

$$\rho\frac{\partial \boldsymbol{q}}{\partial t} + \rho\,\boldsymbol{\nabla}\cdot(\boldsymbol{q}\boldsymbol{q}/\epsilon) + \epsilon\boldsymbol{\nabla}p - \epsilon\rho\boldsymbol{g} - \mu\nabla^2\boldsymbol{q} + \mu F(\epsilon, d, Re_{qd})\boldsymbol{q} = \boldsymbol{0}. \tag{7}$$

This equation, together with the continuity equation (5) and suitable boundary conditions for q, now presents the means to calculate the flow field analytically or numerically, provided the factor F can be explicitly expressed in terms of known parameters. The factor $F(\epsilon, d, Re_{qd})$ represents quantification of the microscopic frictional effects of the

porous matrix on the permeate. It will therefore differ from structure to structure and, through the Reynolds number, its magnitude also depends on the average fluid velocity. The distance d denotes the length scale of the microstructure and may loosely be taken as the average distance between neighbouring particles, void channels or foam strands.

The first term of (7) may be left out in cases of time-independent average motion. For most practical water seepage phenomena like flow through membranes or subsurface groundwater flow the average inertial effects are negligible so that the second term may also be dropped. Inclusion of the gravity term in the pressure term, yielding a total pressure head p then reduces equation (7) to

$$\epsilon \nabla p - \mu \nabla^2 \boldsymbol{q} + \mu F(\epsilon, d, Re_{qd}) \boldsymbol{q} = \boldsymbol{0}. \tag{8}$$

The second term, often called the 'Brinkman term' in international literature, governs the shear stress induced by the average velocity variable $\boldsymbol{q}$ and thus has limited influence in practical problems of water seepage. It is, however, used in large scale numerical simulations of flow to provide a link between the internal flow field in the computational domain and the boundary conditions imposed. One part of this project was to show the possible errors created by incorrect use of these boundary conditions.

If we further restrict the analysis to a uniform seepage velocity

$$\boldsymbol{q} = q\boldsymbol{i} \tag{9}$$

equation (8) reduces to

$$-\epsilon \frac{dp}{dx} = \mu F(\epsilon, d, Re_{qd}) q \tag{10}$$

The functional dependence of F on the parameters ϵ, d and Re_{qd} forms the cornerstone of flow through porous media, since it is this factor F that determines the hydrodynamic permeability of any medium. In fact, according to the definition of hydrodynamic permeability, it follows that

$$K = \frac{\epsilon}{F}. \tag{11}$$

The major part of this project centred around the improvement of models to determine F for various cases of practical interest to water research in South Africa.

In case of isotropic media the evaluation of the drag factor F may be done in accordance with the original proposal by Du Plessis and Masliyah, 1988, namely to introduce a Representative Unit Cell (RUC), allowing the quantitative and qualitative evaluation of all the different contributions to the drag on the fluid explicitly in terms of the porosity ϵ, the scale length d of the microstructure, the type of microstructure through the tortuosity χ and the seepage velocity $\boldsymbol{q}$. The effective cross-sectional area of a single pore is given by the relation

$$A_p = \frac{\epsilon d^2}{\chi}. \tag{12}$$

Consistent herewith the relation between the seepage velocity $\boldsymbol{q}$ and the mean pore velocity $\boldsymbol{v}_p$ is given for all subsequent models by

$$\boldsymbol{v}_p = \frac{\chi}{\epsilon}\boldsymbol{q}. \tag{13}$$

This relation determines the pore velocity uniquely, from which intrapore fluid dynamical phenomena may be deduced accurately. The tortuosity thus takes a prominent place in the modelling and a search for a sound definition of this seemingly simple concept took a major part of the project effort.

4 RESEARCH RESULTS

4.1 Contaminant transport and dispersion

The transport of contaminants in porous media and the dispersion of concentration gradients may to a large extent be classified as either diffusion dominated or convection dominated. In the diffusive case the molecular motion contributes much more to the mixing than the actual flow of the fluid. Conversely, convective dispersion (also referred to as mechanical dispersion) is driven primarily by the the sweeping motion of fluid particles which carry with them the contaminant or tracer. The mechanics of the latter of type of dispersion depends to a large extent on the velocity field of the fluid phase present in the void channels of the porous matrix and the present project is devoted to analyses and prediction of such velocity fields for porous media of practical interest to water science and technology.

4.1.1 Tortuosity

It is commonly found in international literature that dispersion effects are being quantified in terms of dispersion coefficients. This practice has, however, not yet led to satisfactory definitions of these coefficients. Dispersion coefficients determined on the laboratory scale also do not seem to be adequate for use on the field scale and much effort is lost by having to redetermine coefficients for each practical case. One aim of this research project was therefore to investigate the possibility of describing dispersion in a novel manner, starting from an idealized interstitial velocity field $\boldsymbol{v}$, which in turn must be functionally dependend on the average fluid discharge rate $\boldsymbol{q}$ through the porous medium of porosity ϵ. This latter link was proved to be that given in equation (13) where the tortuosity χ is a measure of the tortuousness of the interstitial fluid streamlines. The porosity is usually determinable by experiment and provides no serious problem. It is apparent that knowledge about the tortuosity, and especially about its functional dependence on the porous microstructure, is therefore crucial towards effectively modelling any velocity-dependent flow phenomena. An extensive literature study revealed that, although a seemingly simple concept, there is internationally still widespread confusion on correct definitions and interpretations of tortuosity.

This matter was taken up with Professor Jacob Bear of the Technion in Israel and several months of cooperation as well as some joint research at ETH in Switzerland resulted in a manuscript on efforts to resolve this problem (Du Plessis and Bear, 1995). In short the problem boils down to one school advocating that the tortuosity as such should include all

dynamical effects caused by the tortuous streamlines whereas the other school considers the tortuosity as to present only some average ratio of the actual streamline lengths to the average streamwise displacements. These two tortuosities may be referred to respectively as the *dynamic tortuosity* and the *geometric tortuosity* and in the present work the term tortuosity will refer to the latter type unless stated otherwise. This geometric tortuosity is also sometimes referred to as the *tortuosity factor*.

When referral is made in literature to tortuosity special care must be taken to verify which of the following tortuosities is intended:
Dynamic tortuosity
Geometrical tortuosity
Electric tortuosity
Acoustic tortuosity.

4.1.2 Tracer Dispersion

If no molecular diffusion is allowed in an incompressible fluid environment, the concentration ω of a tracer species is interstitially governed by

$$\frac{\partial \omega}{\partial t} + \nabla\cdot(\omega \boldsymbol{v}) = 0. \tag{14}$$

Volumetric averaging of Equation (14) leads to:

$$\frac{\partial \Omega}{\partial t} + \frac{1}{\epsilon}\nabla\cdot(\Omega \boldsymbol{q}) + \nabla\cdot\frac{1}{V_0}\iiint_{V_f}(\omega - \frac{\Omega}{\epsilon})(\boldsymbol{v} - \frac{\boldsymbol{q}}{\epsilon})\, dV = 0. \tag{15}$$

Another factor of importance is the ratio γ of the fluid velocities v_t and v_p being respectively the actual cross sectional mean velocities in transverse and streamwise pore sections of the RUC:

$$\gamma \equiv \frac{v_t}{v_p}. \tag{16}$$

The factor γ is assumed to be a known constant for each different pore structure (Diedericks, 1992).

The last term on the LHS of equation (15) is known as the flux of mechanical dispersion and provides information on the convective spread of tracer superposed on the average convective motion. This term should therefore give rise to all mechanical dispersion coefficients for the cases under observation. It consists of the volume average of the product of deviations of the velocity and tracer concentration. In its present form this last term is undetermined and for closure some information regarding the porous medium is needed.

Tracer dispersion may be defined as the diffusive effect of non-linearities in the actual intrapore velocity field on a non-linearity in the volumetrically averaged tracer concentration Ω. The effect of tracer dispersion thus manifests itself in a change of average concentration gradient.

A traditional simplification in the modelling of dispersion is the assumption that the dispersive transport is locally governed by a diffusive or Fickian relationship which, in turn, asserts that the flux of mechanical dispersion is proportional to the average concentration gradient. The coefficient of proportionality has been studied extensively for many years and is currently accepted (Tompson and Gray, 1986) as being a second order tensor dependent on the average velocity, $\boldsymbol{q}$, and characteristics of the porous medium. It should therefore be possible to establish the following relationship:

$$\boldsymbol{\nabla}\cdot\frac{1}{V_0}\iiint_{V_f}(\omega-\frac{\Omega}{\epsilon})(\boldsymbol{v}-\frac{\boldsymbol{q}}{\epsilon})\,dV \;=\; \boldsymbol{\nabla}\cdot\underline{\underline{D}}\cdot\boldsymbol{\nabla}\Omega, \tag{17}$$

with the assumption that

$$\underline{\underline{D}} \;=\; a_T q\underline{\underline{I}} \;+\; (a_L - a_T)\frac{\boldsymbol{qq}}{q}. \tag{18}$$

The transverse and longitudinal dispersivity coefficients, respectively a_T and a_L, are determined empirically and as a consequence suffer from experimental inconsistencies (Moltyaner, 1989). It is therefore beneficial to quantify these coefficients directly from pore-scale parameters. For the special case of uniform flow and where the selected reference frame, determined by $\boldsymbol{q}$, coincides with the principle axes of $\underline{\underline{D}}$, it follows that

$$\boldsymbol{\nabla}\cdot\underline{\underline{D}}\cdot\boldsymbol{\nabla}\Omega \;=\; D_L\nabla^2_{\parallel}\Omega \;+\; D_T\nabla^2_{\perp}\Omega. \tag{19}$$

Due to the isotropy condition imposed the volume integral in Equation (17) may be taken over the total volume V_o of the RUC. Thereupon the divergence operator may be

taken inside the integral, since V_o is independent of spatial location (Bear and Bachmat, 1991, Hassanizadeh and Gray, 1979). The divergence theorem is used to transform the volume integral to a surface integral over the six plane surfaces of the RUC, namely:

$$\nabla \cdot \frac{1}{V_0} \iiint_{V_f} (\omega - \frac{\Omega}{\epsilon})(v - \frac{q}{\epsilon})\, dV \;=\; \frac{1}{V_0} \iint_{S_{fs}} (\omega - \frac{\Omega}{\epsilon})(v - \frac{q}{\epsilon}) \cdot \nu \, dS. \tag{20}$$

Exchange of tracer material across each of these interfaces with hypothetically adjacent RUC's may now be determined. Since such exchanges are assumed to take place only convectively, the domain of the surface integral is restricted to these fluid-fluid interfaces of the RUC where the scalar product in the integrand yields non-zero values.

Such an analyses of transverse dispersion, due to convective mixing between adjacent cells, yields (Diedericks, 1992) a dispersion coefficient D_T, in accordance with Equation (19) proportional to the average velocity q, namely

$$D_T \;=\; a_T \frac{q}{\epsilon} \;=\; \left(\frac{\gamma A_p}{2\chi d}\right) \frac{q}{\epsilon} \tag{21}$$

where A_p denotes the cross-sectional area of a single pore. It follows that the factor a_T is of the order of the magnitude of a single pore as suggested by Bear and Bachmat, 1991. It should be noted that Equation (21) is generally applicable to any isotropic porous microstructure.

Experimental verification of this result proved very problematic, since, in all reports on experimental work on transverse dispersion, only the measured dispersion coefficient is given, but not the microstructural parameters. This total lack of fully documented experimental data prompted the research into high porosity foams for which dispersion results may be obtained abroad. Analytical studies were thus aimed at an investigation into the physics of flow in isotropic and anisotropic foams. This study is now completed with substantial comparisons with experiment pointing to the success of the modelling effort. The next stage would be the utilization of this analytical results to predict dispersion phenomena in foams for cases of known experimental dispersion measurements.

4.2 Electrokinetic effects of ions on motion

Activities planned to model electrokinetic effects were scaled down to allow more time for the tortuosity effort. This was done since the motion of ions is closely linked to the interstitial velocity field and hence it was considered more appropriate to await more rigorous results on tortuosity before spending to much effort prematurely on this aspect.

4.3 Influence of structure and pore diameter distribution

The theoretical modelling for discharge of Newtonian fluids through porous media of different structures was extended to include inertial effects caused by interstitial recirculation in foams and prismatic structures. The results were tested against published results and also against experiments conducted cooperatively in France.

The hydrodynamic permeabilities for the different structures are expressed in deterministic form as functions of length parameters and porosity. The resulting average permeability for any given pore diameter distribution for any of the basic structures and for any laminar velocity may therefore be calculated directly. The particular distribution function has of course a physical origin and cannot be born out by mathematics alone. It must be provided by analysis of the specific material under consideration.

4.3.1 Foam Structures

Consolidated porous media in spongelike form were modellled by an RUC containing three mutually orthogonal duct sections of square cross-section. The relationship between the rectangular pore width d_p and the characteristic length d of the microstructure is given by:

$$d_p = \sqrt{\frac{\epsilon}{\chi}} d \tag{22}$$

The tortuosity for such a pore representation is given by (Du Plessis, 1992a):

$$\frac{1}{\chi} = \frac{3}{4\epsilon} + \frac{\sqrt{9-8\epsilon}}{2\epsilon} cos\left[\frac{4\pi}{3} + \frac{1}{3} cos^{-1}\left\{\frac{8\epsilon^2 - 36\epsilon + 27}{(9-8\epsilon)^{3/2}}\right\}\right]. \tag{23}$$

The shear stress factor F is given by (Du Plessis & Masliyah, 1988):

$$F = \frac{1}{d^2}\,\frac{36\chi(\chi-1)}{\epsilon} + \frac{Re_{qd}}{d^2}\,\frac{2.05\chi(\chi-1)}{\epsilon(3-\chi)}. \tag{24}$$

The critical Reynolds number which indicates the transition between Darcy and Forchheimer flow behaviour is given by

$$(Re_{qd})_c = \frac{36(3-\chi)}{2.05}. \tag{25}$$

In case of low Reynolds number flow the hydrodynamic permeability is given by

$$K = \frac{\epsilon d^2}{36\chi(\chi-1)} \tag{26}$$

See Figure 1 for a comparison of these theoretical results with experimental measurements. The success of the analytical results is evident. The present results were published (Du Plessis, Montillet, et al, 1994) and also compared to a model by Comiti and Renaud, 1989, an exercise proving that the present modelling is to be preferred. Although the model by Comiti and Renaud also appears to be a pore-scale model it does make use of a curve fit through experimental data so that the results should inevitably be good. The model seems to break down, however, when the pore-scale geometry and physics are analyzed carefully.

4.3.2 Granular Structures

The RUC introduced for granular structures consists of a cubic volume with a cubic solid placed centrally within and with faces aligned, Du Plessis and Masliyah, 1991. The tortuosity of the porous microstructure is then given by

$$\chi = \frac{\epsilon}{1-(1-\epsilon)^{\frac{2}{3}}} \tag{27}$$

and the scale length of the granules by

$$d_s = (1-\epsilon)^{\frac{1}{3}} d. \tag{28}$$

Evaluation of the non-linear dependence of F on the specific discharge q was done by the modelling interstitial flow recirculation. According to this analysis the factor F is given by

$$F = \frac{36}{d^2} \frac{(1-\epsilon)^{\frac{2}{3}}}{\left[1-(1-\epsilon)^{\frac{1}{3}}\right]\left[1-(1-\epsilon)^{\frac{2}{3}}\right]} + \frac{(1-\epsilon)^{\frac{2}{3}}}{\left[1-(1-\epsilon)^{\frac{2}{3}}\right]^2} \cdot \frac{Re_{qd}}{d^2} \tag{29}$$

with a critical Reynolds number of

$$(Re_{qd})_c = \frac{36\left[1-(1-\epsilon)^{\frac{2}{3}}\right]}{\left[1-(1-\epsilon)^{\frac{1}{3}}\right]}. \tag{30}$$

The hydrodynamic permeability is given in such a case by

$$K = \frac{\epsilon d^2}{36(1-\epsilon)^{\frac{2}{3}}}\left[1-(1-\epsilon)^{\frac{1}{3}}\right] \cdot \left[1-(1-\epsilon)^{\frac{2}{3}}\right]. \tag{31}$$

These equations predict the Ergun equation almost exactly in the range for which the latter are reported to be applicable as is explicitly demonstrated in Figure 2. The Ergun equation was empirically constructed as the average result from a vast range of experimental results for packed beds, conducted over several decades. As the present result for granular media match the Ergun equation in the applicable range it also correctly predicts pressure gradients for packed beds, yielding it unnecessary to conduct new sets of experiments. These results were published (Du Plessis, 1994).

In case of low porosity constraints the equations may be simplified extensively (Du Plessis and Roos, 1993, 1994a). If equation (29) is subject to a condition of low porosity and D is the grain particle diameter it simplifies to

$$FD^2 = \frac{180}{\epsilon^2}(1-\epsilon)^2 + \frac{1.8}{\epsilon^2}(1-\epsilon)Re_{qD} \tag{32}$$

A packed bed, consisting of almost spherical granules of diameter D, will have a porosity near 0.38 yielding a friction effect of:

$$FD^2 = \frac{162}{\epsilon^2}(1+3,6\epsilon) + \frac{1.9}{\epsilon^2}(1-\epsilon)Re_{qD} \tag{33}$$

and this yields a hydrodynamic permeability of:

$$K = \frac{\epsilon^2 D^2}{180}. \tag{34}$$

4.4 Influence of porous structure anisotropy

Of considerable importance for the prediction of flow phenomena in synthetic membrane systems is the effects of anisotropy of the porous matrix. A considerable effort was therefore devoted to this problem and specifically to the capability of the model to predict experimental results. Towards this end, one of the group members, Mr Gerhardus Diedericks spent several weeks at an institution in France to get hands-on experience in an active laboratory cooperating on this problem.

As it is almost impossible to conduct controlled experiments on a microscale, a set of experiments was done on flow through a knitted wire plug of known physical dimensions and structure. The model described above for an isotropic foam structure is straightforwardly generalized to an anisotropic foam of material length scales $d_{(1)}$, $d_{(2)}$ and $d_{(3)}$ and uniform solid strands of cross-sectional area d_s^2.

The only remaing factor to be determined is the particular drag coefficient c_d corresponding to the particular form of the strands of the wire plug used in the experiment. This was determined to be $c_d = 1,32$, owing to the "wire" being formed by two round intertwined wires, and yields the following expression for the pressure gradient corresponding to flow in the 1-direction:

$$-\frac{dP}{dx_1} = \frac{6\mu\chi q d_s}{\epsilon^2 V_o}\left(\frac{4(d_{(2)}-d_s)+(d_{(1)}-d_s)}{(d_{(3)}-d_s)} + \frac{4(d_{(3)}-d_s)+(d_{(1)}-d_s)}{(d_{(2)}-d_s)} + \frac{(d_{(2)}-d_s)^2+4(d_{(2)}-d_s)(d_{(3)}-d_s)+(d_{(3)}-d_s)^2}{(d_{(1)}-d_s)^2}\right)$$

$$+\frac{(d_{(2)}-d_s)^3+(d_{(3)}-d_s)^3}{2(d_{(1)}-d_s)(d_{(2)}-d_s)(d_{(3)}-d_s)}\Bigg)$$

$$+\frac{c_d\rho\chi^2q^2d_s}{2\epsilon^3V_o}\left(d_{(2)}+d_{(3)}-2d_s\right). \qquad (35)$$

In Figure 3 this result is graphically compared to experimental results and to the prediction should the structure be approximated by the isotropic model. It is evident that the improvement obtained by introducing anisotropy is remarkable and that the extra effort is worth while towards accuracy of predicting experimental results. It is interesting to note that the model of Comiti as mentioned above was unable to provide a prediction for this experimental exercise, a fact which adds to the practical usefulness of the present type of modelling.

The tortuosity problem was also attacked locally in an effort to provide a universal definition of a geometric tortuosity tensor which will be suitable for anisotropic media. This work was very successful in that a sound theoretical basis for the pure geometric tortuosity was founded. Although not of direct practical interest, and thus beyond the direct scope of the project, this result does serve as proof that the modelling concepts introduced previously are indeed correct.

4.5 Numerical simulation techniques

The numerical simulation techniques used were improved as the project progressed. An analysis was conducted to determine whether a novel numerical procedure, the so-called non-staggered procedure of Rhie and Chow, 1986, will positively influence the numerical simulation of flow in porous environments. This study entailed the writing of a second two-dimensional code, incorporating a non-staggered grid system, and subsequently a painstaking analysis of checks and balances as the two codes are being run for identical physical problems. The current notion is that the SIMPLEC method, already employed for several years is still superior for flow simulation in porous environments (Patankar, 1980, and Van Doormaal and Raithby, 1984). The technical detail of this work falls outside the realm of this report.

A three-dimensional code was written incorporating the same principles. Loss of key personel towards the end of the project, however, caused a premature ending of this activity and the code is currently not yet operational.

4.6 Macroscopic Boundary Effects

A major practical implication of the project is the generation of transport equations fit for use in computational simulation of porous flow phenomena of practical interest in water research. The computational simulation of complex flow phenomena is, however, dramatically influenced by the boundary conditions imposed on the mathematical problem. A problem arises because the transport equations which govern the flow well within the boundaries of the domain does not hold at external boundaries or at interfaces where abrupt changes in porosity or structure occur. This may cause solutions that appear correct, but do not convey the actual conditions found in laboratory or field experiments.

As a case study to determine the magnitude of possible errors the flow through a granular packed bed bounded by a solid wall was analysed.

Convective heat transfer and also many other transfer phenomena depend quantitatively on the velocity gradient of the fluid normal to the surface across which the transfer phenomenon takes place. It is therefore of cardinal importance to be able to predict the velocity profile near to any internal or containing wall as accurately as possible. In the case of a wall containing a packed bed, as is the case in many chemical reactors, this problem is indeed awkward, since the evaluation of real intrapore velocities is a formidable task. Even the use of the average fluid discharge through a cross-sectional element is not at all straight-forward. The deviation from a uniform average velocity profile through a packed bed may also markedly contribute to the dispersion of solute concentrations. This in turn may adversely affect the determination of dispersion coefficients.

This report comparatively describes two solution methods used to quantify the near-wall velocity distribution in packed beds namely a variational approach and a control-volume discretization approach. The origin of channelling effects is an increase in porosity and if the latter can be quantified, knowledge may be obtained about flow conditions near the container wall.

4.6.1 Spatial variation in porosity

It has been observed experimentally (Roblee *et al.*, 1958, Benenati and Brosilow, 1962) that the average velocity in a packed bed is not uniform as is often assumed, but reaches a peak velocity at approximately one particle diameter from the container wall. This is due to the variation in porosity due to the specific packing arrangement of granules near the wall. For particles of highly irregular shape the porosity is unity at the wall and stabilizes at the average porosity at about one particle radius from the wall (Roblee

et al., 1958). For regular shaped particles such as spheres, the variation in porosity takes the form of a damped oscillatory wave, with oscillations damped out at 4.5 to 5 sphere diameters from the wall, with a minimum at about one sphere radius from the wall (Benenati and Brosilow, 1962) as shown in Figure 4. The porosity in the interior of such a randomly packed bed has been measured as about 0.38 whereas the average porosity for large randomly packed beds of uniform spheres was found to be about 0.39 (Benenati and Brosilow, 1962).

Vortmeyer and Schuster, 1983 and Cheng and Vortmeyer, 1988, have used a bed porosity of 0.4 and approximated the spatial variation in porosity by

$$\epsilon(y) \;=\; \epsilon_b \left[1 + \exp\left(-2\frac{y}{D}\right)\right] . \tag{36}$$

In Figure 4 this approximation is shown for $\epsilon_b = 0.38$. Unless stated otherwise, this will be used throughout in the report in order to obtain results similar to those of Vortmeyer and Schuster, 1983. It should be noted, however, that more realistic approximations to the experimental observations may easily be incorporated into both the solution methods described below.

Vortmeyer and Schuster, 1983, considered spherical particles with diameter D , and for comparison of their analysis with the granular model described above, D can be related to the linear dimension d of the cubic RUC through

$$d \;=\; \left[\frac{\pi}{6\ (1-\epsilon)}\right]^{\frac{1}{3}} D \ , \tag{37}$$

or to the cubic particle side width through

$$d_s \;=\; \left(\frac{\pi}{6}\right)^{\frac{1}{3}} D \ . \tag{38}$$

Transformation of d and Re_{qd} in Equations (28) and (29) to D and Re_{qD} respectively, yields the following:

$$FD^2 \;=\; \frac{55.42\,(1-\epsilon)^{\frac{4}{3}}}{\left[1-(1-\epsilon)^{\frac{1}{3}}\right]\left[1-(1-\epsilon)^{\frac{2}{3}}\right]} + \frac{1.24\,(1-\epsilon)}{\left[1-(1-\epsilon)^{\frac{2}{3}}\right]^2} Re_{qD} \ . \tag{39}$$

In macroscopic continuum theory the porosity is normally defined as a volumetric average taken over a three-dimensional representative elementary volume. For the present study, however, it is required to describe the variation in porosity with respect to the normal distance from the wall. This is accomplished by taking the average porosity over infinitely thin sheets parallel to the wall. If y represents the normal distance from the wall into the bed, this porosity will therefore yield a function $\epsilon(y)$ as is schematically shown in Figure 5. The momentum equation (8) thereupon simplifies to the following for uni-directional flow between parallel plates in the x-direction:

$$\epsilon\frac{\partial p}{\partial x} - \mu\frac{\partial^2 q}{\partial y^2} + \mu q F = 0 \ . \tag{40}$$

For flow in a tube, Equation (8) simplifies to:

$$\epsilon\frac{\partial p}{\partial x} - \mu\left(\frac{\partial^2 q}{\partial r^2} + \frac{1}{r}\frac{\partial q}{\partial r}\right) + \mu q F = 0 \ . \tag{41}$$

It should be noted that the equations above are expressed in terms of D and not d, since the latter scale length will vary with changes in ϵ across the bed. The particle dimension D, however, remains constant, the variation in porosity being caused by changes in packing density only.

Equations (40) and (41) may be rewritten in the following manner:

$$\frac{dp}{dx} = -f_1 q - f_2 q^2 + \mu\frac{d^2 q}{dy^2} \tag{42}$$

and

$$\frac{dp}{dx} = -f_1 q - f_2 q^2 + \mu\left(\frac{d^2 q}{dr^2} + \frac{1}{r}\frac{dq}{dr}\right) \tag{43}$$

where the functions f_1 and f_2 are given by:

$$f_1 = \frac{\mu}{D^2}\cdot\frac{55.42\,(1-\epsilon)^{\frac{4}{3}}}{\left[1-(1-\epsilon)^{\frac{1}{3}}\right]\left[1-(1-\epsilon)^{\frac{2}{3}}\right]} \tag{44}$$

and

$$f_2 = \frac{\rho}{D} \cdot \frac{1.24(1-\epsilon)}{\left[1-(1-\epsilon)^{\frac{2}{3}}\right]^2} \quad . \tag{45}$$

4.6.2 The Ergun equation

The Ergun equation (Bird *et al.*, 1960) gives, for one-dimensional average flow, an empirical relationship between the pressure gradient and the average velocity in an infinite porous medium. The two-dimensional effect, induced by the frictional effect of macroscopic boundaries on average flow, may be empirically supplemented by addition of the so-called Brinkman-term (Brinkman, 1947). The modified Ergun equation for flow in a packed bed between parallel plates is therefore given by the following elliptic partial differential equation (Benenati and Brosilow, 1962):

$$\frac{\partial p}{\partial x} = -f_1 q - f_2 q^2 + \mu \frac{\partial^2 q}{\partial y^2} \tag{46}$$

subject to the following boundary conditions:

$$\begin{aligned} y = 0: &\quad q = 0 \\ y = \tfrac{b}{2}: &\quad \tfrac{\partial q}{\partial y} = 0 \end{aligned} \tag{47}$$

b is the distance between the plates, and the functions f_1 and f_2 are defined as follows:

$$f_1 = 150\,\mu \frac{(1-\epsilon)^2}{\epsilon^3 D^2} \tag{48}$$

$$f_2 = 1.75\,\rho \frac{(1-\epsilon)}{\epsilon^3 D} \quad . \tag{49}$$

The Ergun equation has evolved from numerous empirical correlations of experimental data and is therefore applicable only to the limited range of experimental porosities. In Figures 6 and 7, however, f_1 and f_2 for the Ergun equation as given by Equations (48) and (49) are drawn for the entire porosity range, as the present application makes use of

porosities up to unity. The empirical constants 150 and 1.75 are frequently adjusted in literature (e.g. Dybbs and Edwards, 1982) to obtain better correlation between equation (46) and experimental results. To conform with the work of Vortmeyer and Schuster, the present values will be retained.

For flow in a tubular packed bed, the modified Ergun equation is similarly given by:

$$\frac{\partial p}{\partial x} = -f_1 q - f_2 q^2 + \mu\left(\frac{\partial^2 q}{\partial r^2} + \frac{1}{r}\frac{\partial q}{\partial r}\right) \tag{50}$$

and subject to the boundary conditions

$$\begin{aligned} r = R: &\quad q = 0 \\ r = 0: &\quad \tfrac{\partial q}{\partial r} = 0 \quad . \end{aligned} \tag{51}$$

4.6.3 Solution Method I: Control-volume discretization method

In this method the computational domain is discretized by spanning the domain with a finite number of grid points. The value of the dependent variable, in this case q, is then only determined at each grid point by solving a set of discretization equations for the control volume surrounding the grid point. These equations are obtained by integrating the partial differential equation, in this case Equation (40) or (41) over every one of the non-overlapping control volumes. The integrals are evaluated by means of piecewise linear profiles expressing the variation of q between grid points (Patankar, 1980).

To illustrate this discretization method, consider the following one-dimensional form of the partial differential equation (40) in rectangular Cartesian coordinates:

$$\frac{d}{dy}\left(\mu\frac{dq}{dy}\right) + S = 0 \tag{52}$$

where

$$S = -\mu F q - \epsilon\frac{dp}{dx} \tag{53}$$

and $\frac{dp}{dx}$ is treated as a negative constant.

If the value of q is to be determined at grid point P and if the neighbouring nodes are denoted by W for West and E for East, and the boundaries of the control volume are denoted by w and e respectively, then integration of Equation (52) over this one-dimensional control volume gives:

$$\left(\mu\frac{dq}{dy}\right)_e - \left(\mu\frac{dq}{dy}\right)_w + \int_w^e S\,dy = 0 \ . \tag{54}$$

As stated above, it is now assumed that q changes linearly over the control volume under consideration. Evaluating the derivatives $\frac{dq}{dy}$ in Equation (54) from this piecewise-linear profile for q, the resulting equation will be:

$$\frac{\mu_e\left(q_E - q_P\right)}{(\delta y)_e} - \frac{\mu_w\left(q_P - q_W\right)}{(\delta y)_w} + \bar{S}\,\Delta y = 0 \tag{55}$$

where $\bar{S}$ is the average value of S over the control volume. This central difference spatial discretization equation may be written in the following form:

$$a_P q_P = a_E q_E + a_W q_W + k \tag{56}$$

where

$$\begin{aligned} a_E &= \frac{\mu_e}{(\delta y)_e} \ , \\ a_W &= \frac{\mu_w}{(\delta y)_w} \ , \\ a_P &= a_E + a_W \quad \text{and} \\ k &= \bar{S}\,\Delta y \ . \end{aligned}$$

In the axisymmetrical case, the one-dimensional flow is described by the following partial differential equation:

$$\frac{1}{r}\frac{d}{dr}\left(\mu r\frac{dq}{dr}\right) + S = 0 \tag{57}$$

where S is given by Equation (53). Integration of Equation (57) over the control volume yields:

$$\left(\mu r\frac{dq}{dr}\right)_e - \left(\mu r\frac{dq}{dr}\right)_w + \int_w^e S dr = 0 \ . \tag{58}$$

Assuming a piece-wise linear profile for q, Equation (58) can be written as:

$$\frac{\mu_e r_e\left(q_E - q_P\right)}{(\delta r)_e} - \frac{\mu_w r_w\left(q_P - q_W\right)}{(\delta r)_w} + \frac{\bar{S}}{2}\left(r_e^2 - r_w^2\right) = 0 \ . \tag{59}$$

Written in the form of Equation (56), the coefficients a_P, a_E, a_W and k are given by:

$$a_E = \frac{\mu_e r_e}{(\delta y)_e} \ ,$$

$$a_W = \frac{\mu_w r_w}{(\delta y)_w} \ ,$$

$$a_P = a_E + a_W \quad \text{and}$$

$$k = \frac{\bar{S}}{2}\left(r_e^2 - r_w^2\right) \ .$$

In the case of flow through a packed bed as described earlier, the fluid dynamic viscosity μ is assumed constant, and therefore $\mu_e = \mu_w = \mu$. The solution for the single array of q_P-values according to the boundary conditions (47) and (51) respectively, is now a straightforward matter as is noted in the section concerning the numerical results.

4.6.4 Solution Method II: Variational method

As shown by Vortmeyer and Schuster, 1983 the problem of solving an elliptic partial differential equation subject to certain boundary conditions may be transformed into the problem of minimizing an integral. This method will be illustrated here by deriving the minimization problems for the Ergun equation given by Equations (46) and (50). The derivation below closely follows the exposition by Vortmeyer and Schuster, 1983 and is included for coherence and to clarify some typographical errors in the original work.

The integral

$$E = hl \int_o^b H(y, q, q')\, dy \tag{60}$$

is sought and must be minimized with H satisfying the Euler equation

$$\frac{\partial H}{\partial q} - \frac{d}{dy}\left(\frac{\partial H}{\partial q'}\right) = 0 \tag{61}$$

under the constraint

$$Q = h \int_o^b q\, dy = \text{constant.} \tag{62}$$

Here $q' = \dfrac{dq}{dy}$, and Q is the prescribed constant volumetric flow rate. For parallel plates, an explicit function H which fulfils the above requirements is derived as follows:

Determination of a function H for Cartesian coordinates.

Consider the elliptic partial differential equation (46):

$$f_1 q + f_2 q^2 - \mu q'' + \frac{\partial p}{\partial x} = 0 \ . \tag{63}$$

The integral

$$E = hl \int_o^b H(y, q, q')\, dy \tag{64}$$

with $Q = h \int_o^b q\, dy$ is sought and must be minimized with H satisfying the Euler equation

$$\frac{\partial H}{\partial q} - \frac{d}{dy}\left(\frac{\partial H}{\partial q'}\right) = 0 \ . \tag{65}$$

Equation (65) may also be written as

$$H_q - H_{q'y} - H_{q'q}q' - H_{q'q'}q'' = 0 \ . \tag{66}$$

Considering Equations (63) and (64) it can easily be seen through comparison of the coefficients of equal derivatives that $H_{q'q'} = \mu$ and $H_{q'q} = 0$.

Through integration it follows from $H_{q'q'} = \mu$ that

$$H_{q'} = \mu q' + A(y, q) \tag{67}$$

and thus that

$$H_{q'y} = A_y(y, q)$$

$$\text{and} \qquad H_{q'q} = A_q(y, q) \ .$$

Since $H_{q'q} = 0$, it follows that $A = A(y)$ and thus that

$$H_{q'y} = A'(y) \ .$$

Integration of Equation (67) yields

$$H = \frac{\mu}{2}(q')^2 + A(y)q' + B(y,q) \ . \tag{68}$$

Differentiation of Equation (68) with respect to q yields

$$H_q = B_q(y,q) \ .$$

The Euler equation (66) can therefore be written as

$$B_q(y,q) - A'(y) - \mu q'' = 0 \ . \tag{69}$$

Considering Equations (63) and (69), it can be seen that:

$$B_q(y,q) - A'(y) = f_1 q + f_2 q^2 + \frac{\partial p}{\partial x} \ . \tag{70}$$

Choosing $A'(y) = 0$ gives $A(y) = C$ and

$$B_q(y,q) = f_1 q + f_2 q^2 + \frac{\partial p}{\partial x} \ . \tag{71}$$

Integrating Equation (71) now yields

$$B(y,q) = \frac{f_1}{2}q^2 + \frac{f_2}{3}q^3 + \frac{\partial p}{\partial x}q + K(y) \ . \tag{72}$$

Any function H satisfying Equation (65) is sought, thus choosing the integration constant $C = 0$ and the integration function $K(y) = 0$ keeps the function H simple, and thus Equation (68) is given by:

$$H = \frac{\mu}{2}(q')^2 + \frac{f_1}{2}q^2 + \frac{f_2}{3}q^3 + \frac{\partial p}{\partial x}q \ . \tag{73}$$

Any multiple of this function will also satisfy the Euler equation (65) so that the following equation satisfies all the requirements:

$$H = 2\frac{dp}{dx}q + f_1 q^2 + \frac{2}{3}f_2 q^3 + \mu\left(\frac{dq}{dy}\right)^2 \quad . \tag{74}$$

The integral to be minimized is therefore:

$$E = hl\int_o^b \left[2\frac{dp}{dx}q + f_1 q^2 + \frac{2}{3}f_2 q^3 + \mu\left(\frac{dq}{dy}\right)^2\right] dy \quad . \tag{75}$$

Considering that $\frac{dp}{dx}$ and $\int_o^b q\,dy$ are constant, spatial discretization of Equation (75) by central differencing yields the following minimization problem:

$$\begin{aligned} N &= lh\sum_{i=1}^{n}\left[\Delta y_i q_i\left(q_i f_1 + \frac{2}{3}q_i^2 f_2\right) + \mu\frac{(\Delta q_i)^2}{\Delta y_i}\right] \\ &= \min \end{aligned} \tag{76}$$

with $\Delta q_i = q_{i+1} - q_i$, $\Delta y_i = y_{i+1} - y_i$ and

$$Q = h\sum_{i=1}^{n} q_i \Delta y_i = \text{constant} \quad . \tag{77}$$

In the case of tubular packed beds, the integral to be minimized is given by:

$$E = 2\pi l\int_o^R H(r,q,q')\,r\,dr \tag{78}$$

$$= 2\pi l\int_o^R I(r,q,q')\,dr \tag{79}$$

with

$$Q = 2\pi\int_o^R qr\,dr = \text{constant} \quad . \tag{80}$$

The function I must satisfy the Euler equation

$$\frac{\partial I}{\partial q} - \frac{d}{dr}\left(\frac{\partial I}{\partial q'}\right) = 0 \ . \tag{81}$$

A function I that satisfies Equation (81) is derived as follows:

Determination of a function I for cylindrical coordinates.

For flow in a tube the partial differential equation to be solved is given by:

$$\mu q'' + \frac{\mu}{r} q' - f_1 q - f_2 q^2 - \frac{\partial p}{\partial z} = 0 \ . \tag{82}$$

The integral to be minimized is given by:

$$E = 2\pi l \int_o^R H(r, q, q')\, r\, dr \tag{83}$$

$$= 2\pi l \int_o^R I(r, q, q')\, dr \tag{84}$$

with $Q = 2\pi \int_o^R qr\, dr$.

A function I is sought that satisfies the Euler equation given by:

$$I_{q'q'} q'' + I_{q'q} q' + I_{q'r} - I_q = 0 \ . \tag{85}$$

The following substitution is implemented for simplification:

$$w(r) = q(r)\, r \tag{86}$$

leaving the integral to be minimized as

$$E = 2\pi l \int_o^R I(r, w, w')\, dr \tag{87}$$

with $Q = 2\pi \int_o^R w\, dr$.

The partial differential equation (82) is now given by

$$\frac{\mu}{r}w'' - \frac{\mu}{r^2}w' + \frac{\mu}{r^3}w - f_1\frac{w}{r} - f_2\frac{w^2}{r^2} - \frac{\partial p}{\partial z} = 0 \ , \tag{88}$$

and the Euler equation by:

$$I_{w'w'}w'' + I_{w'w}w' + I_{w'r} - I_w = 0 \ . \tag{89}$$

Comparison of the coefficients of the second derivative w'' in Equations (88) and (89) yields $I_{w'w'} = \frac{\mu}{r}$. Through integration it follows that

$$I_{w'} = \frac{\mu}{r}w' + A(r,w) \tag{90}$$

and thus

$$I_{w'w} = A_w(r,w) \tag{91}$$

and

$$I_{w'r} = -\frac{\mu}{r^2}w' + A_r(r,w) \tag{92}$$

Integrating Equation (90) yields:

$$I = \frac{\mu}{2r}(w')^2 + A(r,w)w' + B(r,w) \ . \tag{93}$$

Differentiation of Equation (93) gives:

$$I_w = A_w(r,w)w' + B_w(r,w) \ . \tag{94}$$

Considering Equations (88) and (89), it now follows that

$$I_{w'w}w' + I_{w'r} - I_w = -\frac{\mu}{r^2}w' + \frac{\mu}{r^3}w - f_1\frac{w}{r} - f_2\frac{w^2}{r^2} - \lambda \tag{95}$$

where $\lambda = \dfrac{\partial p}{\partial z}$.

Substituting the derivatives of I by the expressions obtained above yields:

$$A_r(r,w) - B_w(r,w) = \frac{\mu}{r^3}w - f_1\frac{w}{r} - f_2\frac{w^2}{r^2} - \lambda \ . \tag{96}$$

Taking $A_r(r,w) = \dfrac{\mu}{r^3}w$ and $B_w(r,w) = f_1\dfrac{w}{r} + f_2\dfrac{w^2}{r^2} + \lambda$, it follows that:

$$A(r,w) = -\frac{\mu}{2r^2}w + C(w) \tag{97}$$

and

$$B(r,w) = \frac{f_1}{2r}w^2 + \frac{f_2}{3r^2}w^3 + \lambda w + K(r) \tag{98}$$

Any function I satisfying the Euler equation (85) is sought, thus assuming for simplicity that the integration functions $C(w) = K(r) = 0$, gives the following expression for I:

$$I = \frac{\mu}{2r}(w')^2 - \frac{\mu}{2r^2}ww' + \frac{f_1}{2r}w^2 + \frac{f_2}{3r^2}w^3 + \lambda w \ . \tag{99}$$

Transforming back to q, yields:

$$I = \frac{\mu}{2}q'(q+q'r) + qr\left(\frac{f_1}{2}q + \frac{f_2}{3}q^2 + \lambda\right) \ . \tag{100}$$

Any multiple of this function will also satisfy the Euler equation (85) so that the following equation satisfies all the requirements:

$$I = \mu q'(q+q'r) + qr\left(f_1 q + \frac{2}{3}f_2 q^2 + 2\frac{\partial p}{\partial z}\right) \ . \tag{101}$$

The minimization problem can thus be written as:

$$N = \pi l \sum_{i=1}^{n} \left[\mu q_i \Delta q_i + \mu r_i \frac{(\Delta q_i)^2}{\Delta r_i} + q_i r_i \Delta r_i \left(f_1 q_i + \frac{2}{3} f_2 q_i^2 \right) \right] = \min \tag{102}$$

with $\Delta q_i = q_{i+1} - q_i$, $\Delta r_i = r_{i+1} - r_i$ and constrained by the condition that

$$Q = 2\pi \sum_{i=1}^{n} q_i r_i \Delta r = \text{constant} \ . \tag{103}$$

Considering the partial differential equations obtained by volume averaging, Equations (40) and (41), the minimization problems obtained through the variational method are identical to those derived above for the Ergun equations, except that μ should be replaced by $\frac{\mu}{\epsilon}$ and f_1 and f_2 are then given by Equations (44) and (45).

4.6.5 Numerical results

In this section the numerical solutions are given for

1. the Ergun equation, using the variational method,
2. the volume averaged equation, using the control-volume discretization method, and
3. the volume averaged equation, using the variational method.

In all cases the flow of air at 25°C was considered, thus the following values were used for the density and the dynamic viscosity:

$$\rho = 1.18 \ \text{kgm}^{-3} \qquad \text{and} \qquad \mu = 0.000018 \ \text{Nsm}^{-2}$$

The number of nodes used for the uniform discretization grid was 120 in all cases considered. The porosity ϵ in the expressions for f_1 and f_2 was substituted by the expression in Equation (36).

The control-volume discretization equations were solved numerically using a FORTRAN-program implementing the Thomas algorithm as described by Patankar (1980) and enhanced by Van Doormaal and Raithby (1984). Every iteration does a forward and a backward sweep across the grid points. Since the present study involves fully developed flow, only one row of nodes is needed to solve for the cross-stream velocity profile, thus simplifying to a one-dimensional problem.

The minimization problems (76) and (102) were solved numerically using the IMSL Math/Library function LCONF (IMSL,1991). This routine is based on M.J.D. Powell's FORTRAN package for linearly constrained optimization calculations TOLMIN. The length of the plates/tube was taken as 10m and $D_B = 40$mm.

In Figures 8 and 9 the flow profiles obtained by the control-volume discretization of the volume averaged equations (40) and (41) respectively are given for $\epsilon_b = 0.4$, $D_B = 40$mm, $D = 2$, 4 and 6mm, and for $Re_{qD} = 5$. It was found that results of methods 1 to 3 above are very much the same and the slight differences cannot be distinguished on a graph. These differences may also be attributed to round-off errors in the numerical procedures.

4.6.6 Experimental correlation

It is very difficult to accurately measure the average flow characteristics inside a packed bed. Experimental data is, however, available for measurements taken a small distance above the bed. Vortmeyer and Schuster, 1983, give a graphical representation of the flow distribution measured 10mm above a fixed bed for air at 25°C with $\epsilon_b = 0.4$, $Re_{qD} = 7.5$ and $D = 2$mm .

In order to compare the results of the volume averaging method with these experimental values, the control-volume discretization method was extended to two dimensions to be able to handle the flow redevelopment above the packed bed. In the x-direction a part of the calculation domain is regarded as porous with porosity as given by Equation (36). Further down-stream the porosity is set to $\epsilon = 1$. The velocity profile is then calculated 10mm into the free-flow regime. The result for a tubular packed bed, using a 51x120 finite volume grid, is given in Figure 10. The measured profile 10mm above the bed as given graphically by Vortmeyer and Schuster (1983) is also shown. These approximate values have been obtained by direct measurements on Figure 12 in Vortmeyer and Schuster, 1983. It can be seen in Figure 10 that the present results based on the cubic RUC model, correspond reasonably with the experimental data.

Vortmeyer and Schuster, 1983, solved the Brinkman equation, extended to higher flow rates by incorporating the Ergun pressure loss relation, by means of a variational method.

Their approximation for the porosity distribution was used throughout this section. There is, however, no guarantee that this approximation will yield the same total discharge as for the original distribution as shown in Figure 4. Both methods of solution discussed above are capable of predicting the flow for the experimental oscillatory porosity distribution, provided a proper distribution function $\epsilon(y)$ or enough data points can be prescribed which match the experimental data.

Du Plessis and Masliyah, 1991, volume-averaged the mass and momentum equations, and by modelling granular porous media through a specific geometrical structure within an RUC, obtained differential equations describing the flow through any granular porous medium. These equations may be solved numerically by means of a control-volume discretization method, or by variational method as used by Vortmeyer and Schuster, 1983, to solve the extended Brinkman equation.

Both solution methods mentioned above, were used. The results are nearly identical, with some differences that may be attributed to round-off errors. Furthermore, these solutions compare favourably with those given by Vortmeyer and Schuster, 1983. It should be noted that the control-volume discretization method is much simpler and quicker than the variational method.

The model for granular porous media (Du Plessis and Masliyah, 1991) applied to packed beds with porosity distribution function as given by Equation (36), yields results that compare favourably with those given by the solution of the extended Brinkman equation (Vortmeyer and Schuster, 1983). This is comforting since the latter equation is purely empirical, while the granular model was derived from physical principles. Further attention is, however, needed regarding the validity of the sheet-wise porosity distribution function.

It was clearly demonstrated that in case of a macroscopic solid boundary within a granular medium, a simple boundary condition implying Darcy flow bounded by slip flow is more accurate for mass flux prediction than the more popular no slip condition which causes viscous losses via the Brinkman term. This work was accepted for publication and will be published shortly (Du Plessis and Roos, 1994c).

4.7 Unsaturated flow

The problem of unsaturated flow is of importance in most soil-related water research. During a visit to the Oregon State University a research seminar was held during which possible cooperation in this field was investigated. In accordance with one of the suggestions arrived at during the seminar it is of paramount importance that the hydrodynamic permeability for fully saturated flow through sandstone was analysed satisfactorily to serve as an asymptotic condition benchmark for unsaturated flow.

A key physical difference between fluid transport in membranes (and foams) and soils is that the porosity in the latter case is extremely small. This fact was already used to substantially simplify expressions for permeability of granular media for conditions of low and very low porosity (Du Plessis and Roos, 1993, 1994a). The results were again extermely encouraging and reported in the Journal of Geophysical Research (Du Plessis and Roos, 1994b).

In literature concerning the permeability of sandstones, the grain size is used as characteristic length. In most cases the grain size is described by the volume diameter, i.e. the diameter of a sphere having the same volume as a particle. If d_g denotes the grain size, the relation between the solid width d_s and d_g is given by

$$d_s = \left(\frac{\pi}{6}\right)^{\frac{1}{3}} d_g \ . \tag{104}$$

In terms of the grain size equation (31) can thus be written as

$$K = \frac{\epsilon d_g^2 \left[1-(1-\epsilon)^{\frac{1}{3}}\right]\left[1-(1-\epsilon)^{\frac{2}{3}}\right]}{63(1-\epsilon)^{\frac{4}{3}}} \ . \tag{105}$$

4.7.1 Massilon sandstone

Massilon sandstone is a Mississippian subarkose with moderately well-sorted and subrounded grains (Green and Wang, 1986. Koplik et al., 1984, give the bulk porosity of Massilon sandstone as 0.22 and the average grain size as 400μm. The bulk permeability was measured as 2.5 darcy, but calculated by means of an effective medium theory coupled with a network of resistors as 27.4 darcy, which is ten times higher than the measured

value. Schlueter et al., 1991, predicted a permeability of 3.1 darcy, also using an effective medium theory, but taking into account the effect of the cross-sectional shape, orientation, and constrictivity of the pores. Green and Wang, 1986, give the average grain size as 200μm and the porosity range as $0.21 - 0.22$. Although the lower limit for the grain size is probably somewhat below $d_g = 200\mu$m, this value is shown in Figure 11 together with the limiting conditions ($d_g = 400\mu$m, $\epsilon = 0.21$ and $\epsilon = 0.22$), the measured and calculated permeability given by Koplik et al., 1984, and the predicted value of Schlueter et al., 1991. For a porosity of 0.22 and a grain size of 400μm, equation (105) gives a permeability of 8.16 darcy.

4.7.2 Berea sandstone

Berea sandstone is a medium-grained, low-rank Mississipian graywacke with well-sorted grains Green and Wang, 1986. The grain size for low-rank graywacke lies between 62.5μm and 250μm. This gives an average grain size of 156.25μm, quite close to the average grain size of 155μm as reported by Green and Wang, 1986. The porosity lies between 0.15 Seeburger and Nur, 1984, and 0.23 Macdonald et al., 1986. Taking the average of this porosity range ($\epsilon = 0.19$) and the average grain size ($d_g = 156.25\mu$m), equation (105) yields a permeability of 0.74 darcy. Schlueter et al., 1991, report the experimentally measured value as 0.46 darcy. In Figure 12 the permeability of Berea sandstone is shown as a function of porosity. The solid lines correspond to the limiting conditions $d_g = 62.5\mu$m, $d_g = 250\mu$m, $\epsilon = 0.15$ and $\epsilon = 0.23$ respectively. Measured permeability values given by Wyllie and Spangler, 1952, and Seeburger and Nur, 1984, as well as calculated values by Seeburger and Nur, 1984, are also shown. Measured and calculated values given by Schlueter et al., 1991, are shown in Figure 12 as straight lines, spanning a range of porosities, since the grain size of the samples was not provided.

4.7.3 Fontainebleau sandstone

Fontainebleau sandstone is made exclusively of well-sorted quartz grains cemented by silica Doyen, 1988. This makes it well-suited for comparison with the results of the pore-scale model for granular porous media. Doyen gives the porosity of Fontainebleau sandstone as between 0.05 and 0.22. The grain size is given as between 150 and 300μm.

In Adler et al., 1990, the permeability is depicted as a function of porosity. The experimental values given in Adler et al., 1990, are shown in Figure 13 together with two lines corresponding to the limiting values for d_g, i.e., 150 and 300μm, and predicted by equation (105). It is clear that the bounds imposed by equation (105) represent very realistic bounds for experiments in the porosity range $\epsilon > 0.08$.

For very small porosities there may be a greater occurrence of blocked throats in the case of near-spherical particles. The pore-scale modelling considers a hypothetical packing of identical cubes and ignores the appearance of blocked throats. This could be the reason for the difference between the calculated permeability and Adler's experimental data in the porosity range $\epsilon < 0.08$.

The rest of this section is devoted to the influence of blocked throats at very low porosities. It should be stressed that what follows is not part of the basic model developed above, but only serves to indicate what the effect of blocked throats would be on the basic results. It is not at all based on physical properties per se, but purely on the available experimental data. The result is interesting, though, and further investigation into the occurrence of blocked throats could prove valuable.

Spearing and Matthews, 1991, have modelled the characteristic properties of sandstone by means of a computer program. Their data is based on Clashac outcrop sandstone which is a relatively clay-free, well characterised rock. According to their Table II, blocked throats begin to occur at a porosity of approximately 0.14. Blocked throats will cause adjacent pores to become passive zones through which fluid is not transported.

In an attempt to quantify the effect of these dead-end pores on the permeability, an effective porosity, ϵ_{eff} is introduced. The porosity at which blocked throats begin to occur will be referred to as the threshhold porosity ϵ_t. The porosity at which all pores are blocked, the cut-off porosity, is denoted by ϵ_c. For porosities greater than the threshhold porosity ϵ_t, ϵ_{eff} will numerically be the same as ϵ. For porosities smaller than the cut-off porosity ϵ_c, ϵ_{eff} will be zero. The objective here is to find a function describing ϵ_{eff} between ϵ_c and ϵ_t. For simplicity, this function of the real porosity ϵ is assumed to take the form of a second-order polynomial to give a gradual decrease below ϵ_t and a complete blocking at ϵ_c. Assuming this polynomial to be of the form

$$\epsilon = a \left[\epsilon_{eff}(\epsilon)\right]^2 + b\,\epsilon_{eff}(\epsilon) + c \ , \tag{106}$$

and by applying the conditions

$$\begin{aligned} \epsilon_{eff}(\epsilon_c) &= 0 \\ \epsilon_{eff}(\epsilon_t) &= \epsilon_t \\ \frac{d\epsilon_{eff}(\epsilon_t)}{d\epsilon} &= 1 \ , \end{aligned}$$

the coefficients a, b, and c are found to be

$$a = \frac{\epsilon_c}{\epsilon_t^2}$$

$$b = 1 - 2\frac{\epsilon_c}{\epsilon_t}$$

$$c = \epsilon_c \ .$$

In Figure 14 the effective porosity is shown as a function of the actual porosity. ϵ_t was taken as 0.14 and ϵ_c as 0.4. The corresponding permeability for Fontainebleau sandstone is indicated in Figure 15 by two lines for $d_g = 150\mu$m and $d_g = 300\mu$m respectively.

It can be seen from Figure 15 that the pore-scale model with the adjustment for blocked throats at very low porosities predicts a very accurate envelope for the experimental permeability values of Fontainebleau sandstone. If throat blocking is indeed the cause of the discrepancy between the present theory and the experimental data of Adler et al., 1990, it would be worth the effort to direct more attention to the determination of the threshhold and cut-off porosities.

The graphical results presented clearly show that almost all the experimental results are captured by the envelopes predicted by equation (105). It was demonstrated that for very low porosities, the influence of blocked throats becomes a major factor in the prediction of the permeability.

The only limitation of the model seems to be the rectangular geometry which appears somewhat different from actual soil and rock formations. The obvious remedy is the introduction of a shape factor, as is done in most other models, but it is evident from the present results that such a relaxation is not needed for sandstone predictions.

5 RESEARCH OUTPUT

Although this project was primarily aimed at the development of mathematical methods for flow phenomena in membrane systems, the generality of the approach allowed diversification to a range of related fields with very promising results. The research output was very satisfactory and a list of novel publications emanating there from is presented below: (see references for details):

1. Du Plessis, 1993b
2. Du Plessis, 1994
3. Du Plessis and Diedericks, 1993
4. Du Plessis, Montillet, et al., 1994
5. Du Plessis and Roos, 1993
6. Du Plessis and Roos, 1994a
7. Du Plessis and Roos, 1994b
8. Du Plessis and Roos, 1994c.

A further point of interest is the tremendous response, especially from the international forum, sparked by the two publications in **WATER SA** (Du Plessis and Roos, 1993, 1994a). This confirms that the work done was of high technical quality and that Water SA is being widely read by researchers abroad. In addition to these publications regarding the work done for this project, the following relevant papers were read at conferences and research seminars:

1. DU PLESSIS, J.P., *Modelling of pressure drop measurements*, Département Génie Chimique, Institut Universitaire de Technologie de Saint-Nazaire, Université de Nantes, Saint-Nazaire, France, June 14, 1993.

2. DU PLESSIS, J.P. & DIEDERICKS, G.P.J., *On tortuosity and areosity tensors in porous media*, 15th Annual Meeting of the Canadian Applied Mathematics Society, Université de Montréal, Montréal, Quebec, Canada, June 6-9, 1994.

3. DU PLESSIS, J.P., & ROOS, L.I., *On boundary conditions in porous media*, Eleventh Canadian Symposium on Fluid Dynamics, Edmonton, Alberta, Canada, June 10-12, 1994.

4. DU PLESSIS, J.P., *Velocity distributions in porous media* Department of Mechanical Engineering, Ecole Polytechnique, University of Montreal, Montreal, Quebec, Canada, June 1994.

5. DU PLESSIS, J.P., *Pore-Scale Modelling of Flow Phenomena in Porous Media*, Department of Bioresource Engineering, Oregon State University, Corvallis, Oregon, USA, June 1994.

6 PROJECT ASSESSMENT

6.1 Fulfilment of Contract Objectives

The prime objective of the project was to further improve the modelling framework for the deterministic mathematical analysis of flow phenomena in porous media and to demonstrate the enhancement of practical predictive capabilities in this field. The construction of the theoretical basis should, however, be done in such a manner that generalization of any aspect may be attempted logically. At initiation of the project the following specific aspects were proposed for special attention:

1. Contaminant transport and dispersion
2. Electrokinetic effects of ions on motion
3. Macroscopic Boundary Effects
4. Influence of Anisotropy of the Porous Structure
5. Membrane Morphology and pore diameter distribution
6. Numerical simulation techniques
7. Unsaturated flow

As is discussed in the report, remarkable progress was obtained in the majority of these aspects and, since all the activities involved research efforts with unkown outcome, this is gratifying. Except for the analysis on electrokinetic phenomena, progress is reported on all aspects considered. Viewed globally the project produced a sound theoretical basis for the analytical and computational quantification of seepage phenomena for foams and granular materials over the entire porosity and velocity spectra. This is of particular importance to research on the enhancement of water purification methods and the study of contaminant transport in groundwater systems.

Contract objectives were thus fulfilled and substantial advances were made in the predicting capabilities of modelling results for a variety of problems in water related research.

6.2 Contributions to the State of Art

A unified theory is being presented by which the same physical and mathematical principles are used to obtain momentum and tracer transport equations for an unlimited range of practically possible porosity and microstructure length scales. The analytical predictive results were shown to be accurate over a porosity range varying from 5% in case of sandstones to 98% for foams. Lengths scales of experimentally verified results varies between a few micrometers for sandstones and several millimeters in case of packed beds.

In addition a variety of basic porous structures can be handled, namely foams, granular media and unidirectional fibre beds.

6.3 Significance of this Report

This report summarizes theoretical results which may be used during the predictive analyses of a great variety of water research problems including microfiltration through synthetic membranes, groundwater, macrofiltration in packed beds and foams.

Although aimed primarily at flow phenomena in synthetic membranes it is shown in this report that all results are directly applicable to several other water related research problems. In fact, since quantification of membrane morphology is so extremely difficult, the verification of the model results was done here through comparison to different porous flow phenomena for which the physical parameters of the microstructure were experimentally determinable.

6.4 Recommendations

This research was done to provide a sound framework towards the prediction of flow and transfer processes in porous media. As such the action needed is further publication of results in technical journals to reach such a wide group of researchers as possible. Especially important is the fact that the results are interdisciplinary applicable and it is hoped that in future this will lead to cross-fertilization between different research communities, thereby cutting down on duplication of costly experimental work.

Further research in this field will aid significantly in broadening the interdisciplinary knowledge base of water science. Typical research fields in need of further development are the following:

1. Tracer dispersion.
   The theory developed in the course of the project has been demonstrated to accurately predict basic hydrodynamical phenomena as observed in nature and on laboratory scale. The underlying knowledge of flow fields must therefore be a reasonable approximation of real life situations and may therefore be used for analysis of tracer transport which may accompany water seepage in aquifers, membrane systems, filtration plants, etc.

2. Prediction of groundwater seepage.
   A novel methodology to predict pinching effects in sandstone formations was developed and shown to be effective in modelling flow disparities in very low porosity sandstones. This seemingly successful method should be investigated further with regard to comparison with more experimental evidence and other microstructures.

3. Electrokinetic effects in porous media.
   This is one aspect in which the project failed to show the anticipated progress and it is believed that, given the progress demonstrated on the other fundamental issues, the way is now paved to put analysis on elecktrokinetica phenomena on the same sound footing.

7 REFERENCES

1. ADLER, P.M., JACQUIN, C.G. & QUIBLIER, J.A. 1990
Flow in simulated porous media, *International Jounal of Multiphase Flow*, vol. 16(4), pp. 691-712.

2. BACHMAT, Y. & BEAR, J. 1986
Macroscopic modelling of transport phenomena in porous media. 1: The continumm approach, *Transport in Porous Media*, vol. 1, pp. 213-240.

3. BEAR, J. & BACHMAT, Y. 1986
Macroscopic modelling of transport phenomena in porous media. 2: Applications to mass, momentum and energy transport, *Transport in Porous Media*, vol. 1, pp. 241-269.

4. BEAR, J. & BACHMAT, Y. 1991
Introduction to Modelling of Transport Phenomena in Porous Media, Kluwer Academic Publishers, Dordrecht, Holland.

5. BENENATI, R.F. & BROSILOW, C.B. 1962
Void fraction distribution in beds of spheres, *A.I.Ch.E. Journal* vol.8, pp. 359-361.

6. BIRD, R.B., STEWART, W.E. & LIGHTFOOT, E.N. 1960
Transport Phenomena, John Wiley, New York.

7. BRINKMAN, H.C. 1947
A calculation of the viscous force exerted by a flowing fluid on a dense swarm of particles, *Appl. Sci. Res.* vol.A1, pp. 27-86.

8. CHENG, P. & VORTMEYER, D. 1988
Transverse thermal dispersion and wall channelling in a packed bed with forced convective flow, *Chemical Engineering Science* vol.43, pp. 2523-2532.

9. CHU, W.-S., STRECKER, E.W. & LETTENMAIER, D.P. 1987
An Evaluation of Data Requirements for Groundwater Contaminant Modeling, *Water Resources Research*, vol. 23(3), pp. 408-424.

10. COMITI, J., & RENAUD, M. 1989
A new model for determining mean structure parameters of fixed beds from pressure drop measurements: application to beds packed with parallelepepidal particles, *Chemical Engineering Science*, vol. 44(7), pp. 1539-1545.

11. DIEDERICKS, G.P.J. 1992
Tracer Dispersion in Porous Media MSc Thesis, Department of Applied Mathematics, University of Stellenbosch, Stellenbosch, South Africa.

12. DOYEN, P.M. 1988
Permeability, Conductivity, and Pore Geometry of Sandstone, *Journal of Geophysical Research*, vol. 93(B7), pp. 7729-7740.

13. DU PLESSIS, J.P., 1993a
Mathematical modelling of flow through porous membranes, Water Research Commission Report No 402/1/93, Pretoria, South Africa.

14. DU PLESSIS, J.P. 1993b
Mathematical modelling and hydrology in a developing region, Proceedings of the 6th South African National Hydrology Symposium, Pietermaritzburg, RSA, September 8-10, 1993, vol. 2, pp. 583-588.

15. DU PLESSIS, J.P. 1994
Analytical quantification of coefficients in the Ergun equation for fluid friction in a packed bed, *Transport in Porous Media*, vol.16. pp. 189-207.

16. DU PLESSIS, J.P. & BEAR, J. 1995
On the tortuosity of isotropic porous media, submitted.

17. DU PLESSIS, J.P., & DIEDERICKS, G.P.J. 1993
On contaminant dispersion in isotropic porous media, in *Water Pollution II - Modelling, Measuring and Prediction*, eds. L.C. Wrobel and C.A. Brebbia, Proceedings of the Second International Symposium on Water Pollution, Milan, Italy, June 21-23, pp. 93-100.

18. DU PLESSIS, J.P. & MASLIYAH, J.H. 1988
Mathematical modelling of flow through consolidated isotropic porous media, *Transport in Porous Media* vol. 3, pp. 145-161.

19. DU PLESSIS, J.P. & MASLIYAH, J.H. 1991
Flow through isotropic granular porous media, *Transport in Porous Media*, vol. 6. pp. 207-221.

20. DU PLESSIS, J.P., MONTILLET, A., COMITI, J., & LEGRAND, J. 1994
Pressure drop prediction for flow through high porosity metallic foams, *Chemical Engineering Science*, vol. 49(21), pp. 3545-3553.

21. DU PLESSIS, J.P., & ROOS, L.I. 1993
Permeability prediction for water seepage through low porosity granular porous media, *Water SA*, vol. 19(2), pp. 147-152.

22. DU PLESSIS, J.P., & ROOS, L.I. 1994a
Improvement on prediction for water seepage through low porosity granular media, *Water SA*, vol. 20(2), pp. 175-178.

23. DU PLESSIS, J.P., & ROOS, L.I. 1994b
Predicting the hydrodynamic permeability of sandstone with a pore-scale model, *Journal of Geophysical Research - Solid Earth*, vol. 99/B10, pp. 19771-19776.

24. DU PLESSIS, J.P., & ROOS, L.I., 1994c
Near-wall channelling in a packed bed, *Engineering Computations*, to be published.

25. DYBBS, A. & EDWARDS, R.V. 1982
A new look at porous media fluid mechanics - Darcy to turbulent, *Proceedings of the NATO Advanced Study Institute on Mechanics of Fluids in Porous Media*, Newark, Delaware, U.S.A., July 18-27.

26. GREEN, D.H. & WANG, H.F. 1986
Fluid pressure response to undrained compression in saturated sedimentary rock, *Geophysics*, vol. 51(4), pp. 948-956.

27. HASSANIZADEH, M. & GRAY, W.G. 1979
General Conservation Equations for Multi-Phase Systems: 1. Averaging Procedure, *Advances in Water Resources*, vol. 2, pp. 131-144.

28. IMSL Math/Library 1991
FORTRAN subroutines for mathematical applications, Version 2.0, September 1991.

29. KOPLIK, J., LIN, C. & VERMETTE, M. 1984
Conductivity and permeability from microgeometry, *Journal of Applied Physics*, vol. 56(11), pp. 3127-3131.

30. MACDONALD, I.F., KAUFMAN, P. & DULLIEN, F.A.L. 1986
Quantitative image analysis of finite porous media. II. Specific genus of cubic lattice models and Berea sandstone. *Journal of Microscopy*, vol. 144, p. 297.

31. MASLIYAH, J.H. 1994
Electrokinetic Transport Phenomena. AOSTRA Technical Publication Series #12, Edmonton, Canada

32. MOLTYANER, G.L. 1989
Hydrodynamic Dispersion at the Local Scale of Continuum Representation, *Water Resources Research*, vol. 25(5), pp. 1041-1048.

33. PATANKAR, S.V. 1980
Numerical Heat Transfer and Fluid Flow, Hemisphere Publishing Corporation, New York.

34. RHIE, C.M., & CHOW, W.L. 1986
Numerical study of the turbulent flow past an airfoil with trailing edge separation, *AIAA Journal* vol. 21(11), pp. 1525-1532.

35. ROBLEE, L.H.S., BAIRD, R.M. & TIERNEY, J.W. 1958
Radial porosity variations in packed beds, *A.I.Ch.E. Journal* vol.4, pp. 460-464.

36. SCHLUETER, E.M., COOK, N.G.W., ZIMMERMAN, R.W. & WITHERSPOON, P.A. 1991
Predicting permeability and electrical conductivity of sedimentary rocks from microgeometry, *Rock Mechanics as a Multidisciplinary Science*, Proceedings of the 32nd U.S. Symposium, The University of Oklahoma,Norman, 10-12 July 1991, pp. 355-364.

37. SEEBURGER, D.A. & NUR, A. 1984
A pore space model for rock permeability and bulk modulus, *Journal of Geophysical Research*, vol. 89(B1), pp. 527-536.

38. SPEARING, M. & MATTHEWS, P. 1991
Modelling characteristic properties of sandstones, *Transport in Porous Media*, vol. 6, pp. 71-90.

39. TOMPSON, A.F.B. & GRAY, W.G. 1986
A Second Order Approach for the Modeling of Dispersive Transport in Porous Media 1. Theoretical Development, *Water Resources Research*, vol.22(5), pp. 591-599.

40. VAN DOORMAAL, J.P. & RAITHBY, G.D. 1984
Enhancements of the SIMPLE method for predicting incompressible fluid flows, *Numerical Heat Transfer* vol.7, pp. 147-163.

41. VORTMEYER, D. & SCHUSTER, J. 1983
Evaluation of steady flow profiles in rectangular and circular packed beds by variational method, *Chemical Engineering Science* vol.38(10), pp. 1691-1699.

42. WYLLIE, M.R.J. & SPANGLER, M.B. 1952
Application of electrical resistivity measurements to problem of fluid flow in porous media, *Bulletin of the American Association of Petroleum Geologists*, vol. 36(2), pp. 359-403.

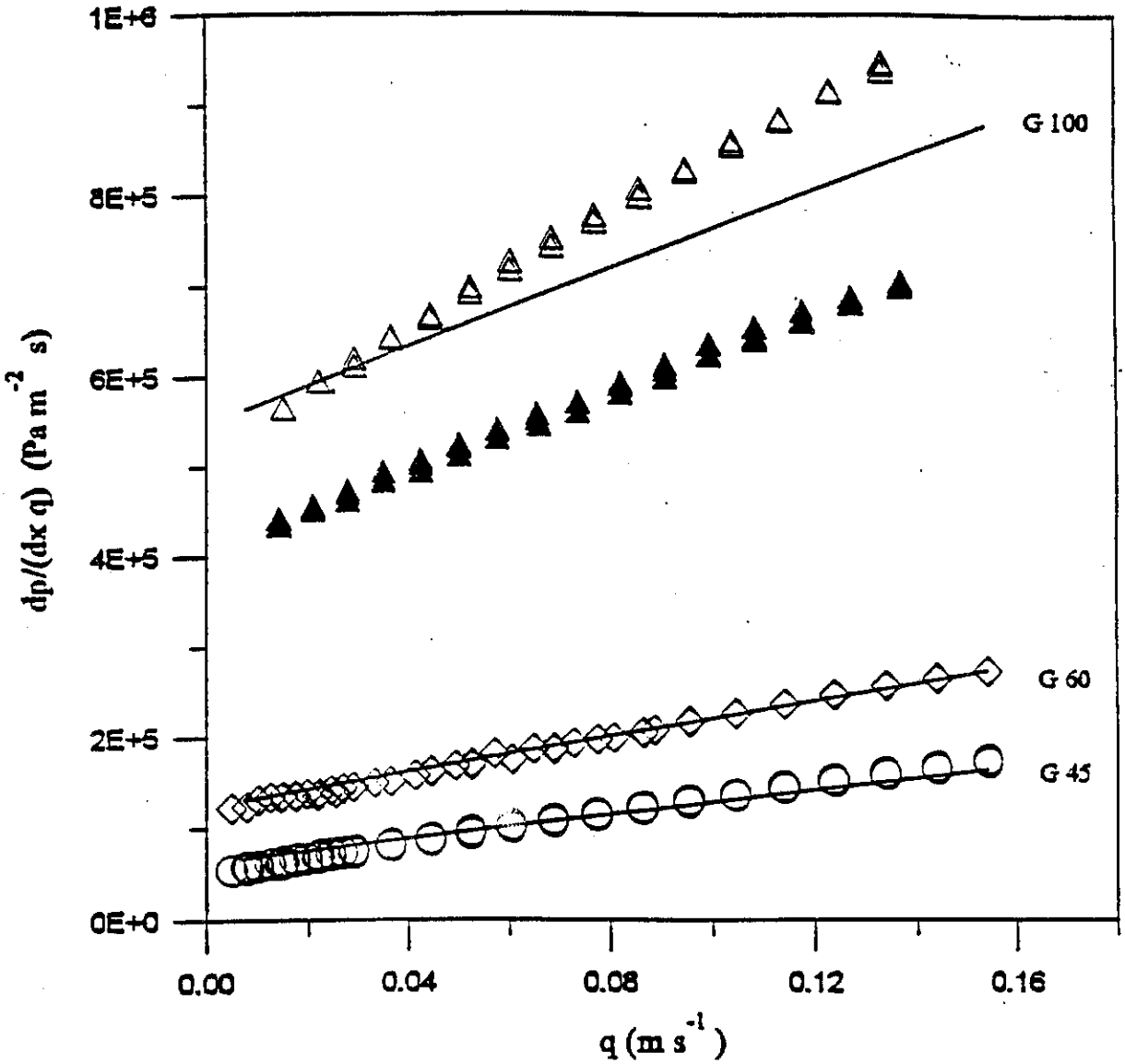

Figure 1: Comparison of results for isotropic foams with the grades (G pores per inch) indicated.

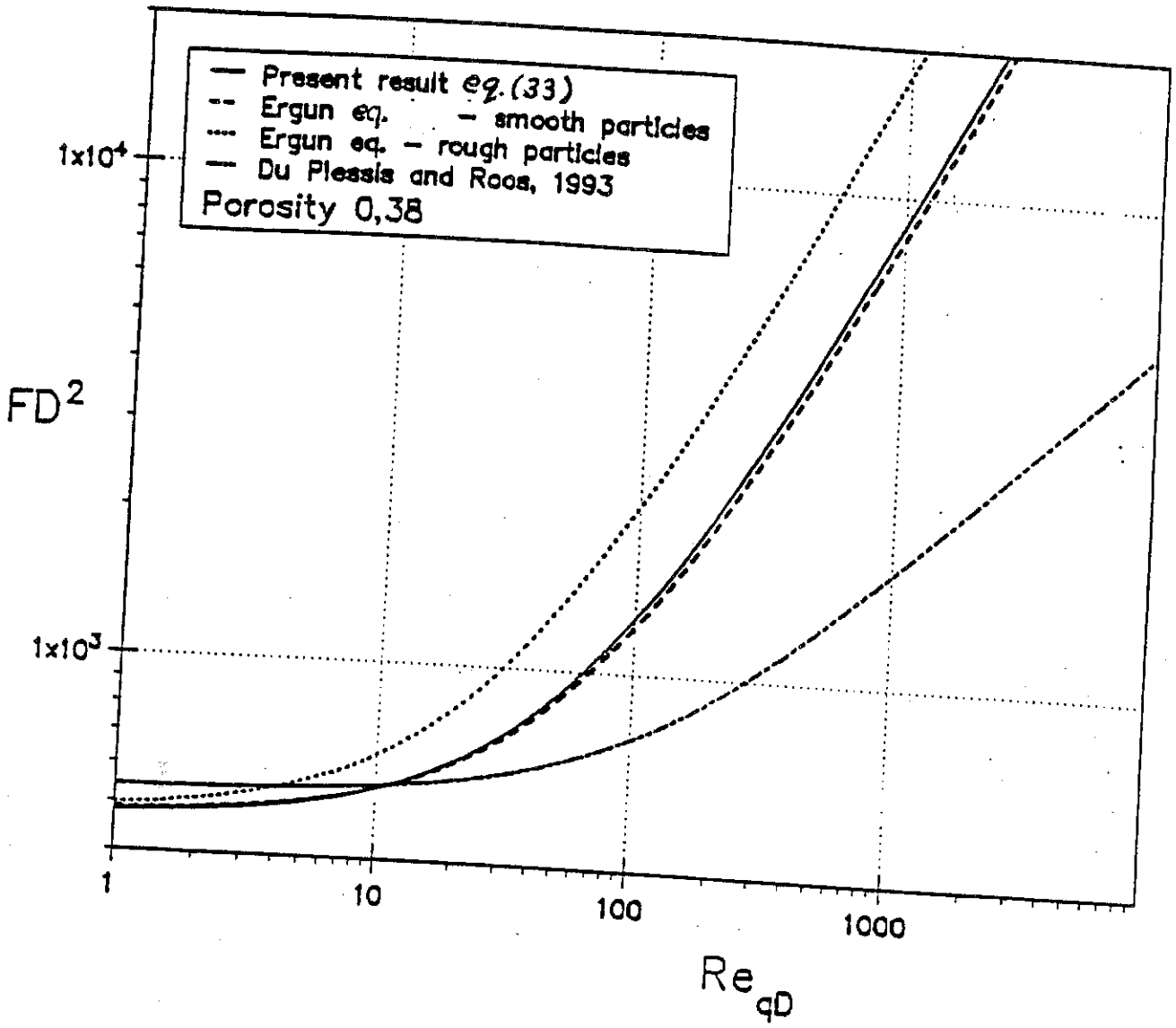

Figure 2: Comparison of results against Ergun equation for granular media.

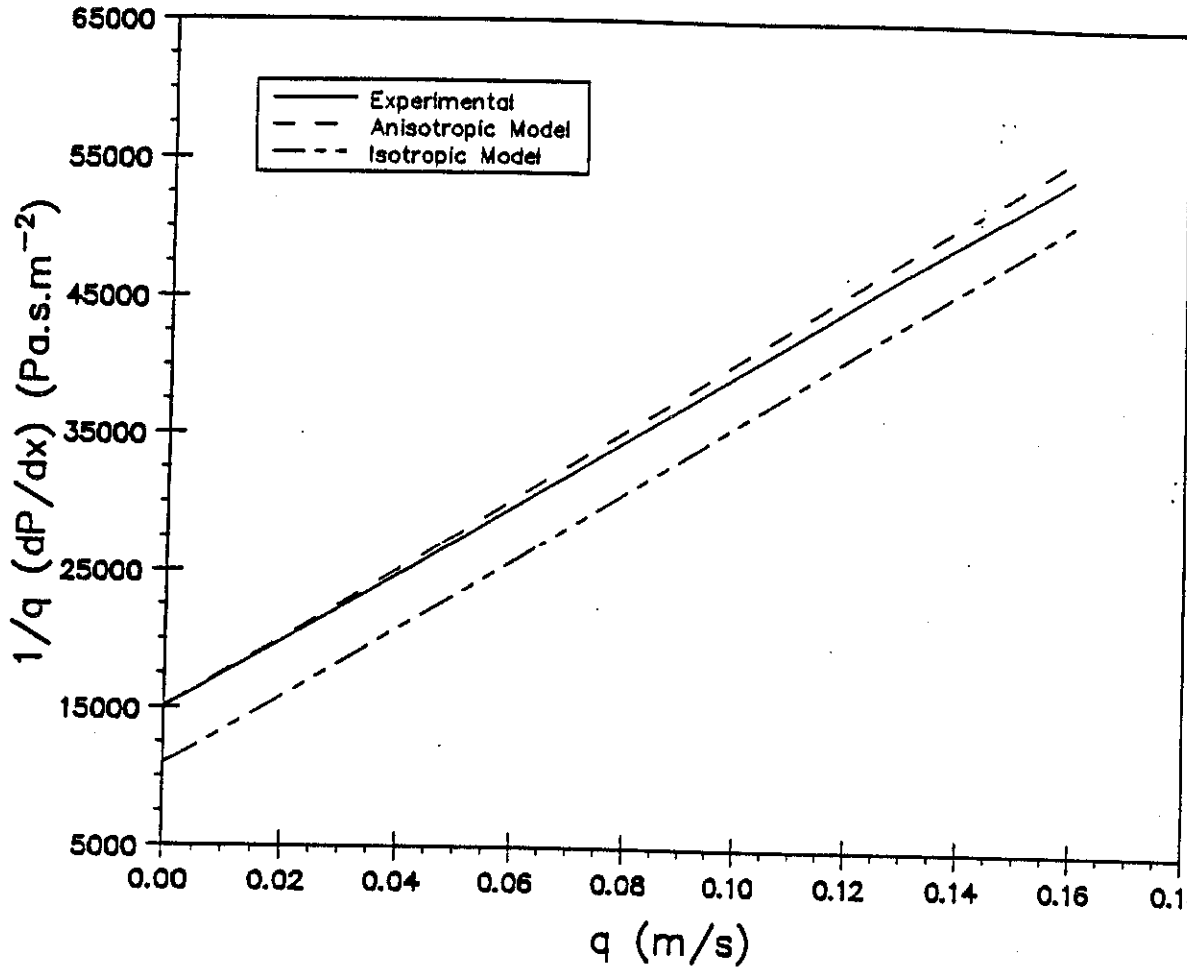

Figure 3: Comparative results for anisotropic foamlike material.

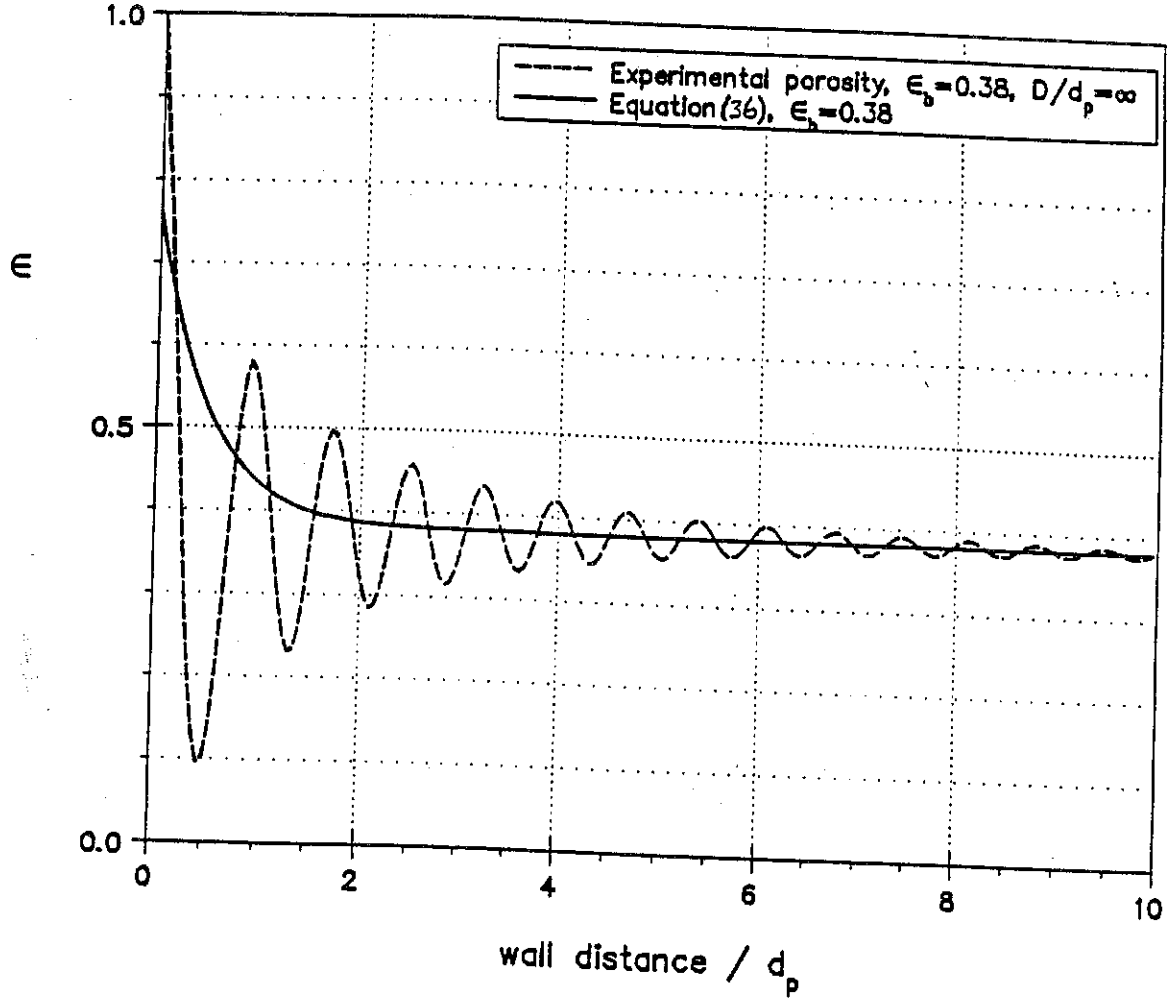

Figure 4: Porosity distribution near external wall.

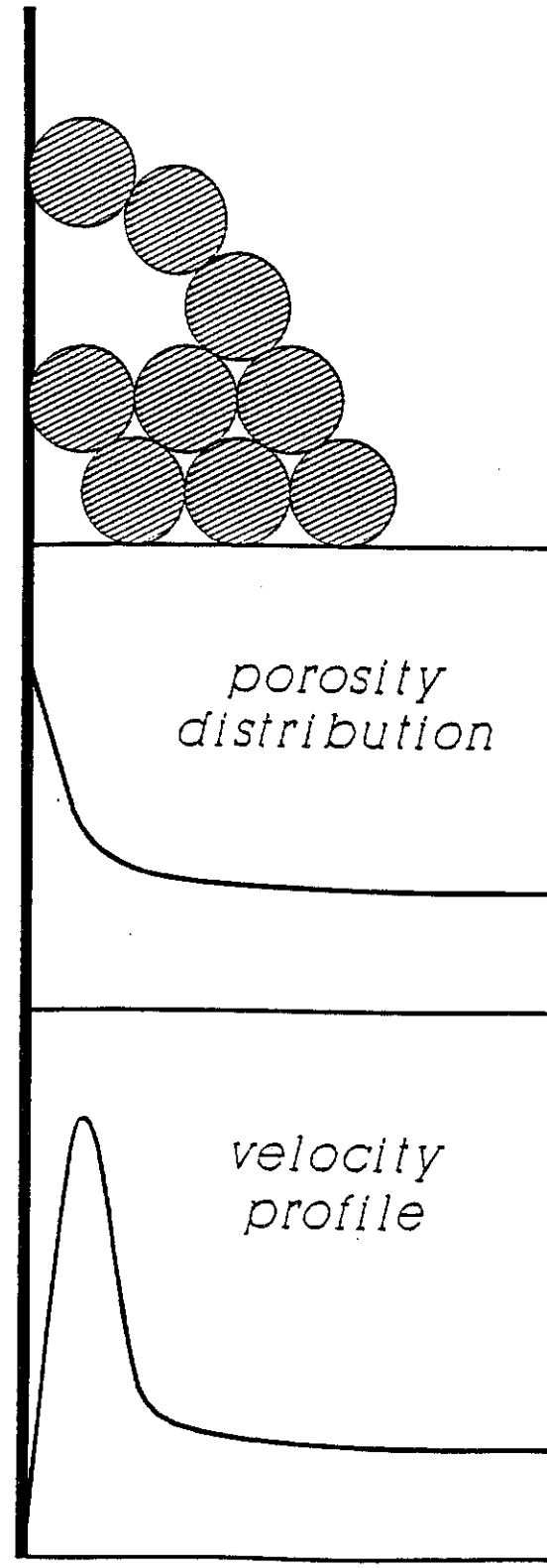

Figure 5: Effects induced by external wall for granular media.

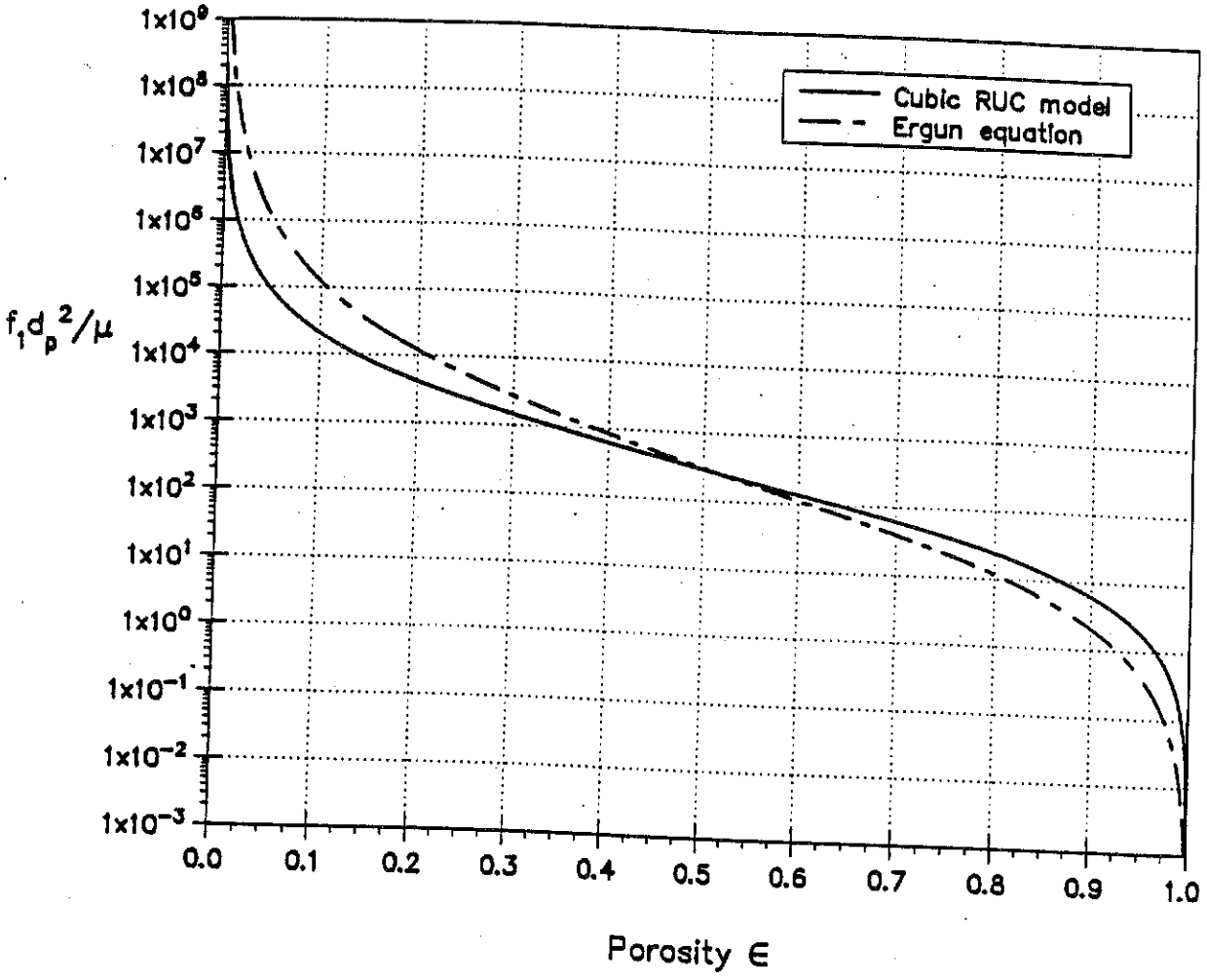

Figure 6: Viscous drag in granular medium.

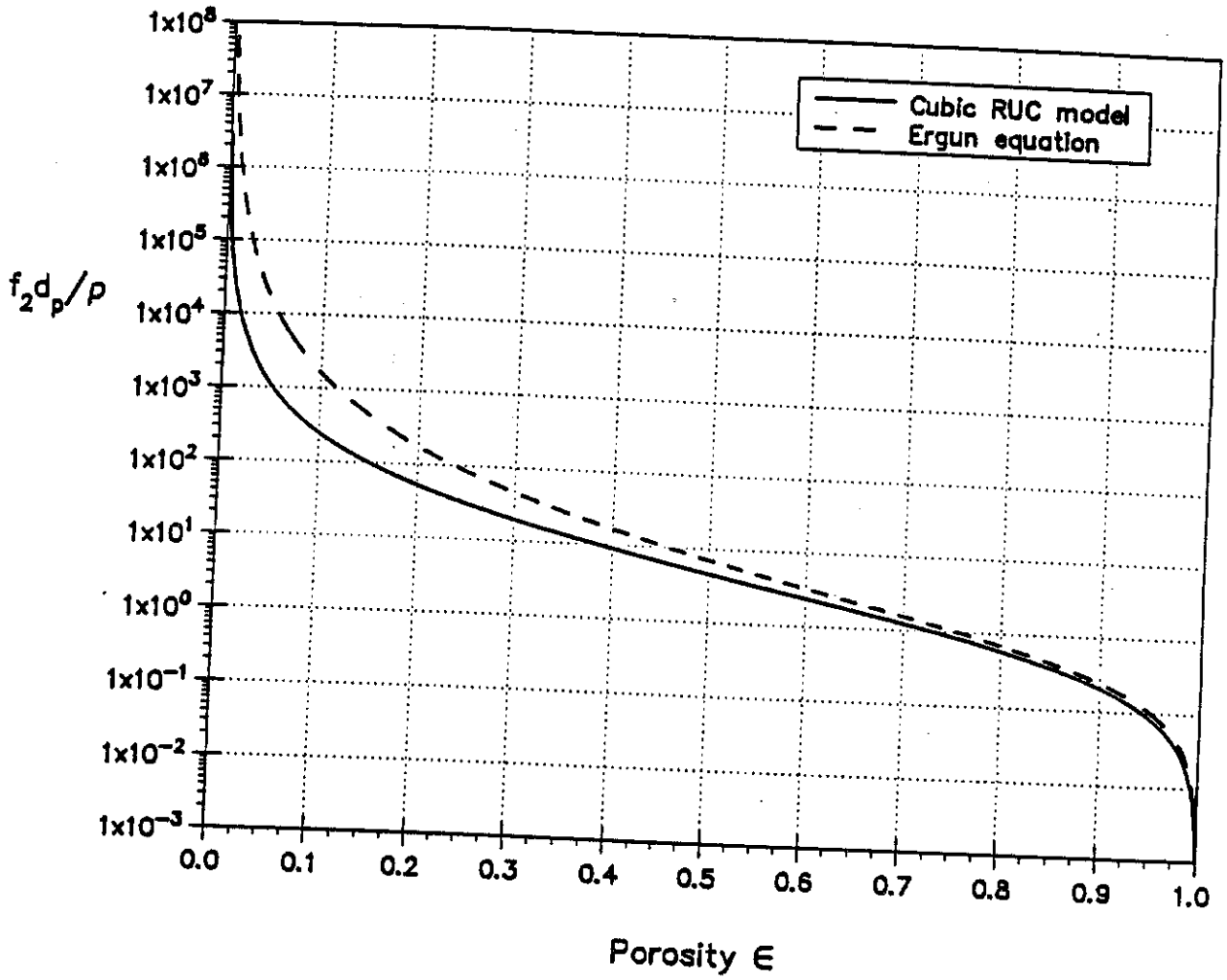

Figure 7: Form drag in granular medium.

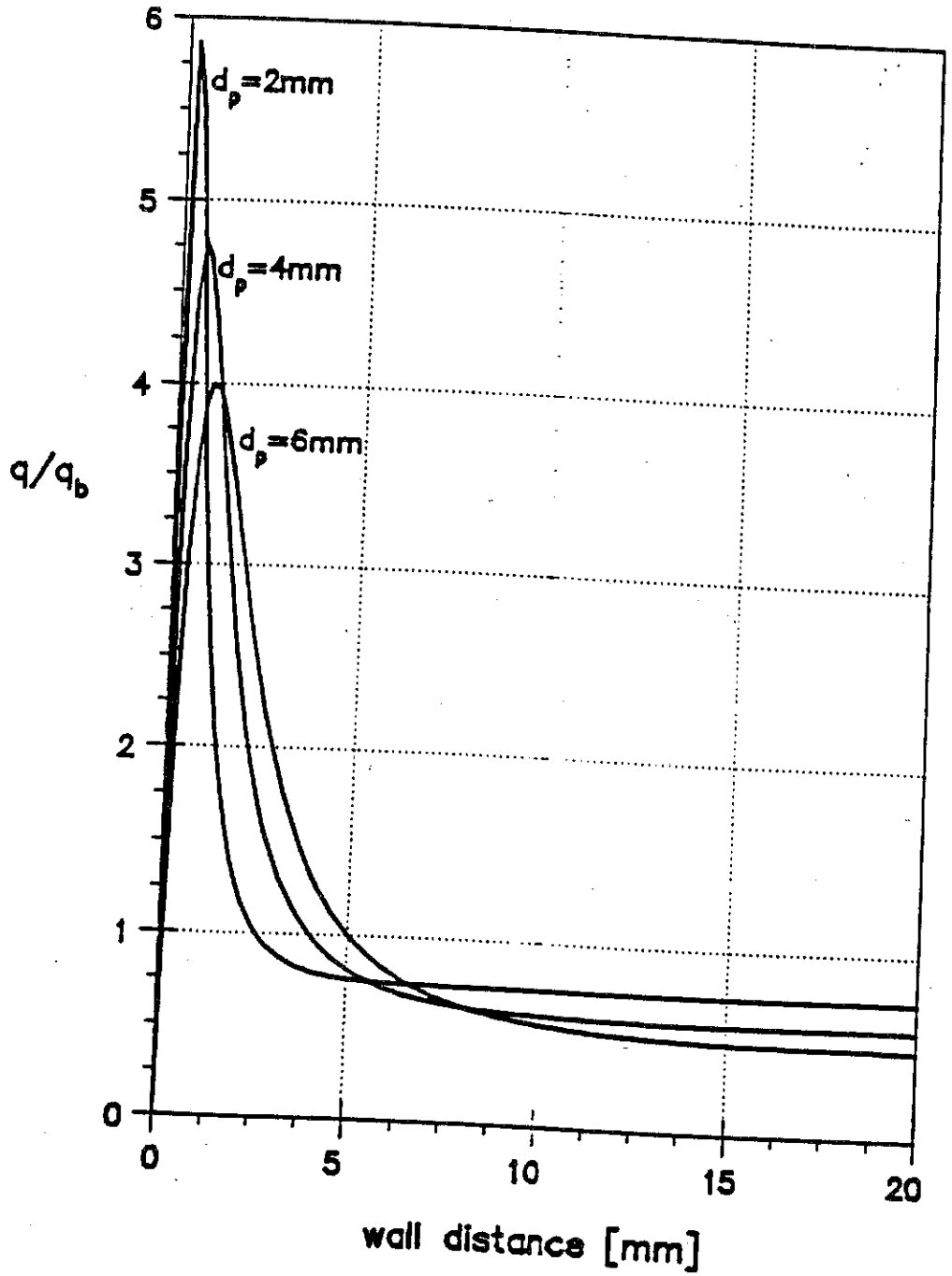

Figure 8: Flow profiles for granuler medium between parallel plates.

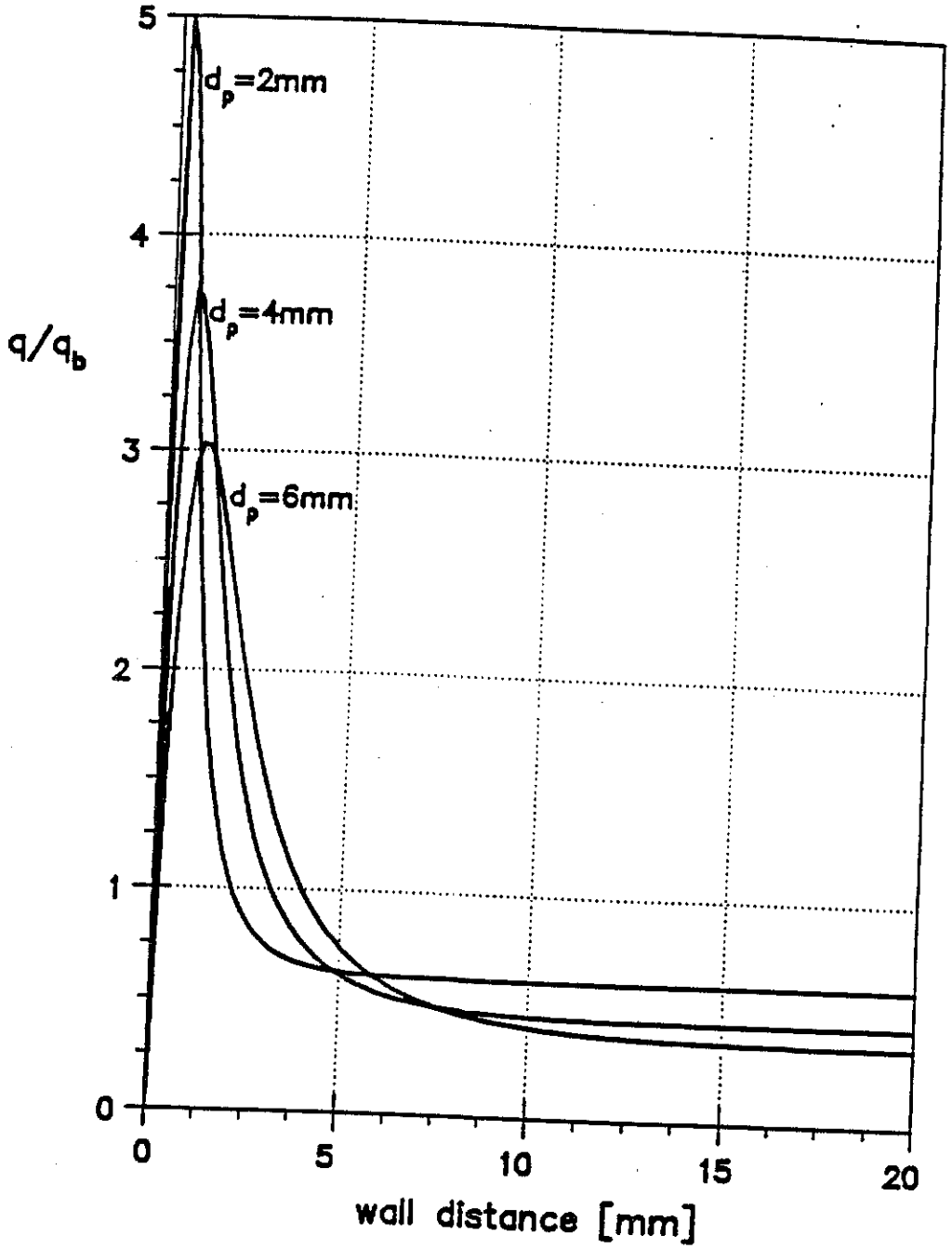

Figure 9: Flow profiles for granular medium in a circular tube

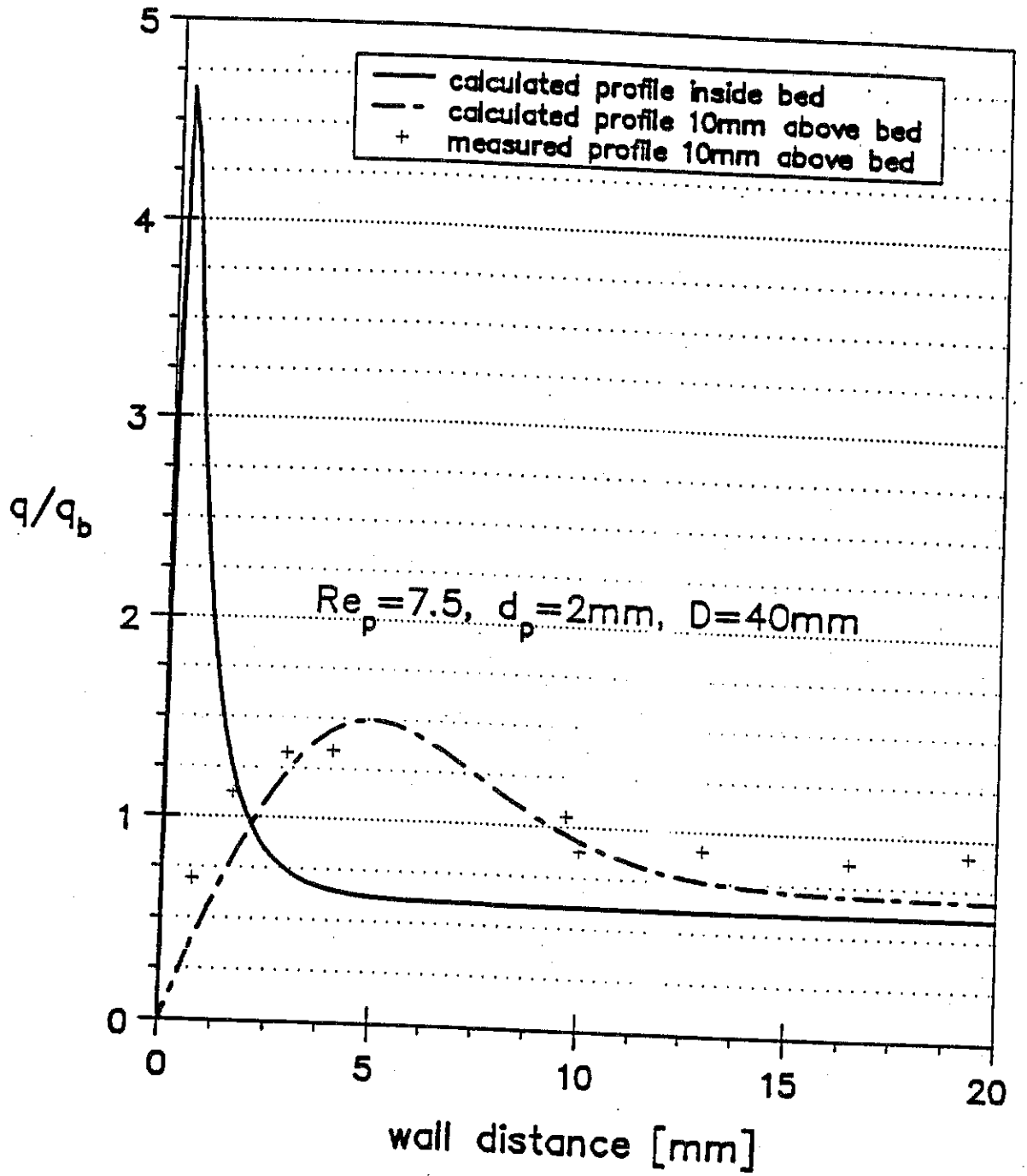

Figure 10: Flow profile inside and 10mm above a tubular packed bed.

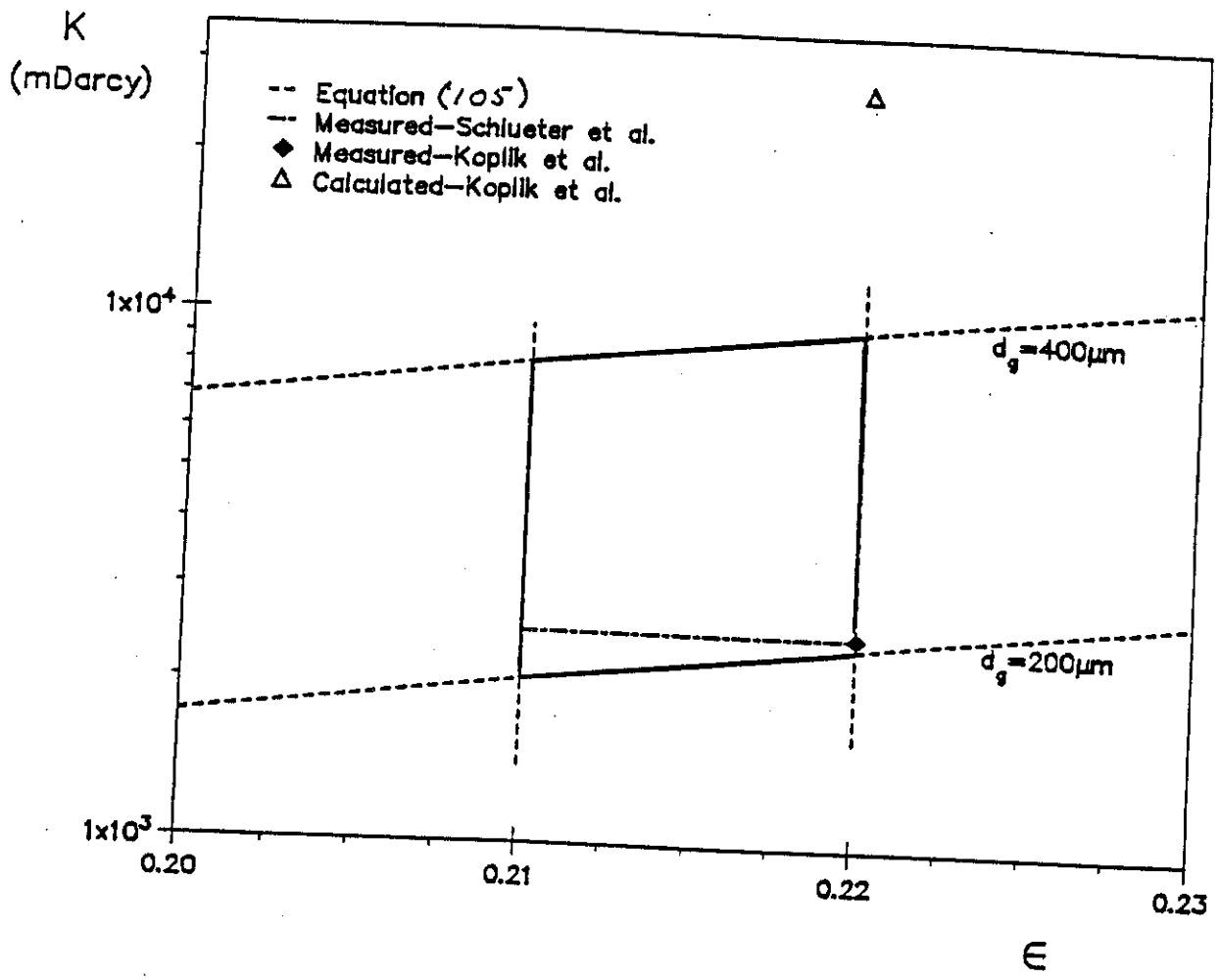

Figure 11: Results for Massilon sandstone.

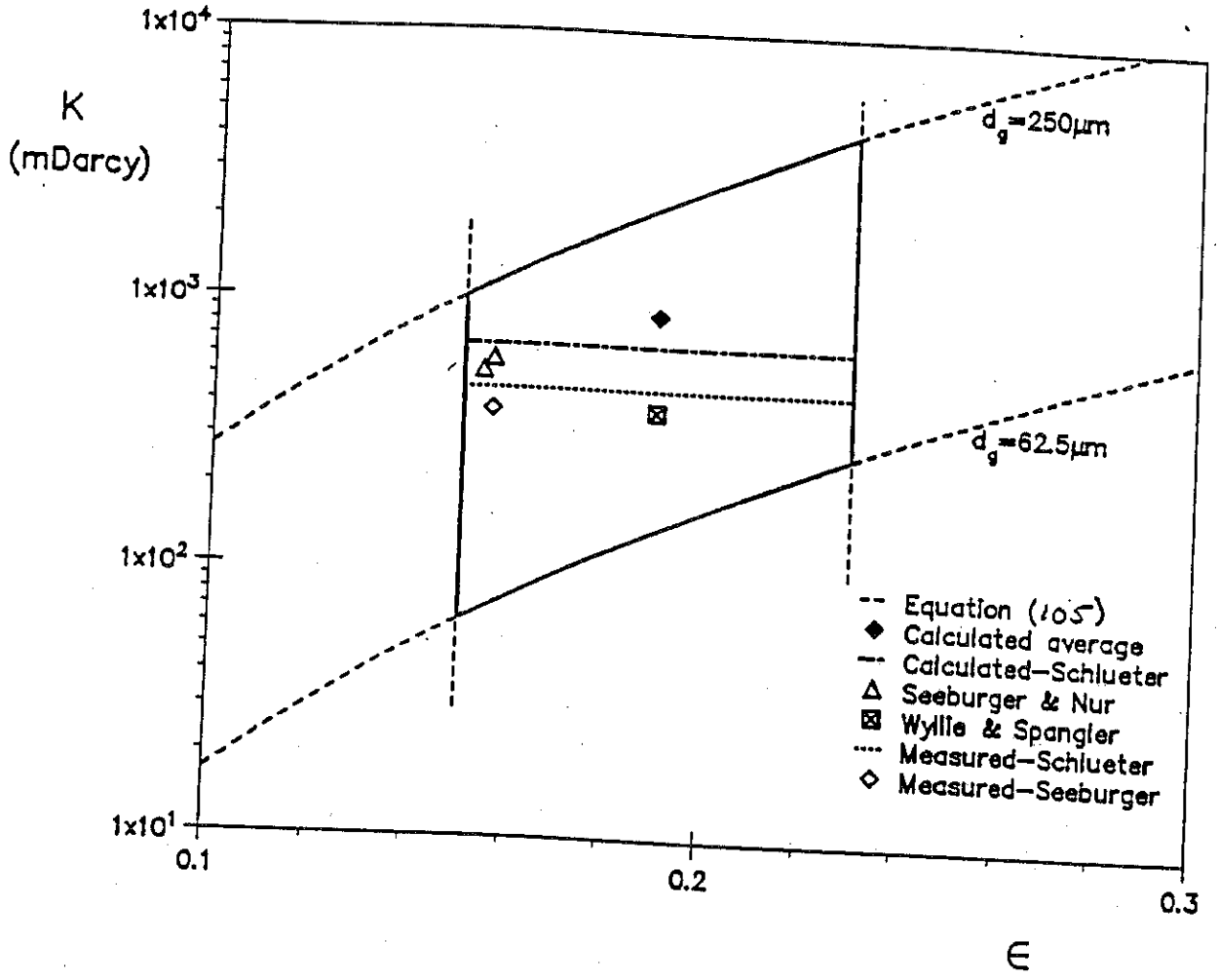

Figure 12: Results for Berea sandstone.

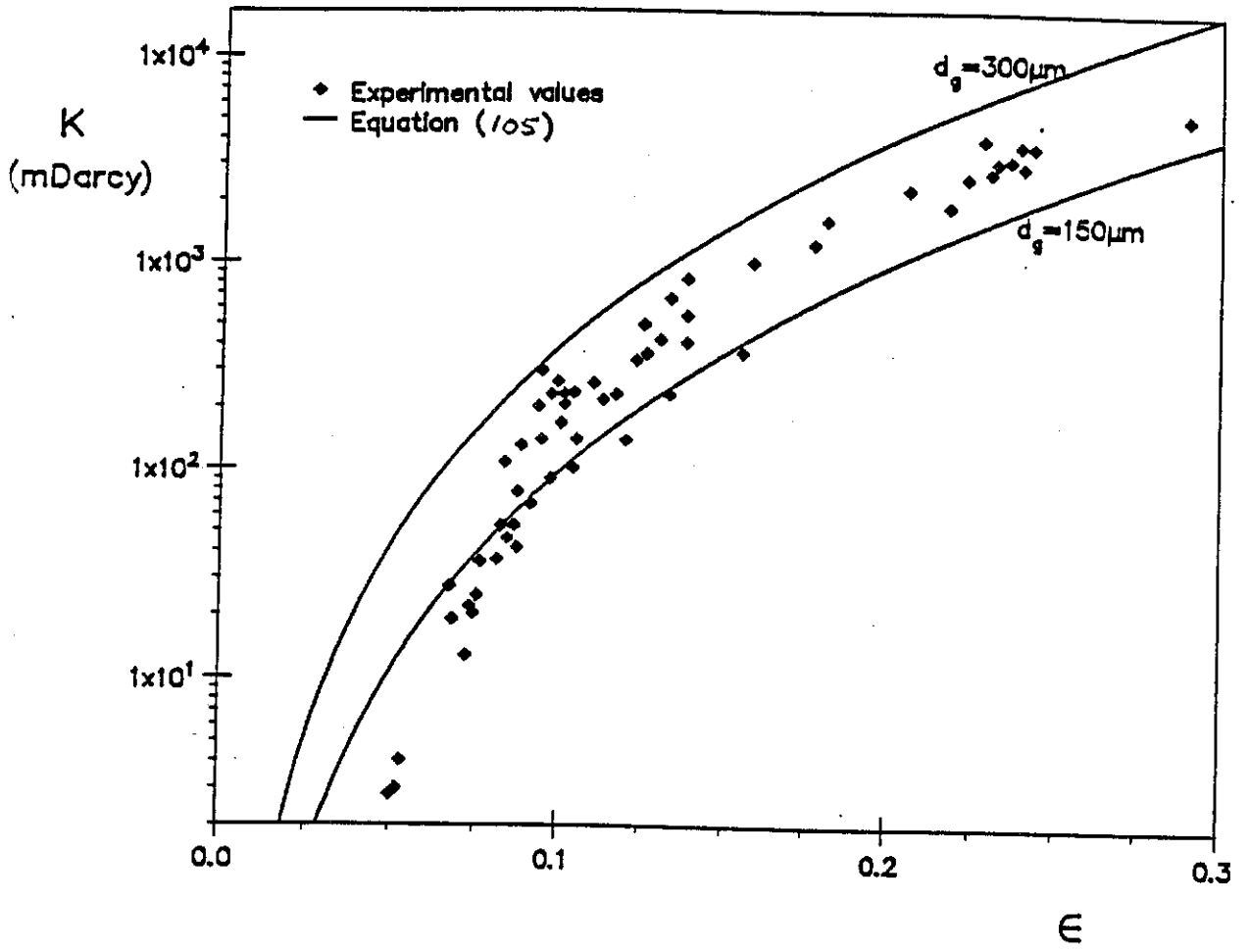

Figure 13: Experimental results for Fontainebleau sandstone.

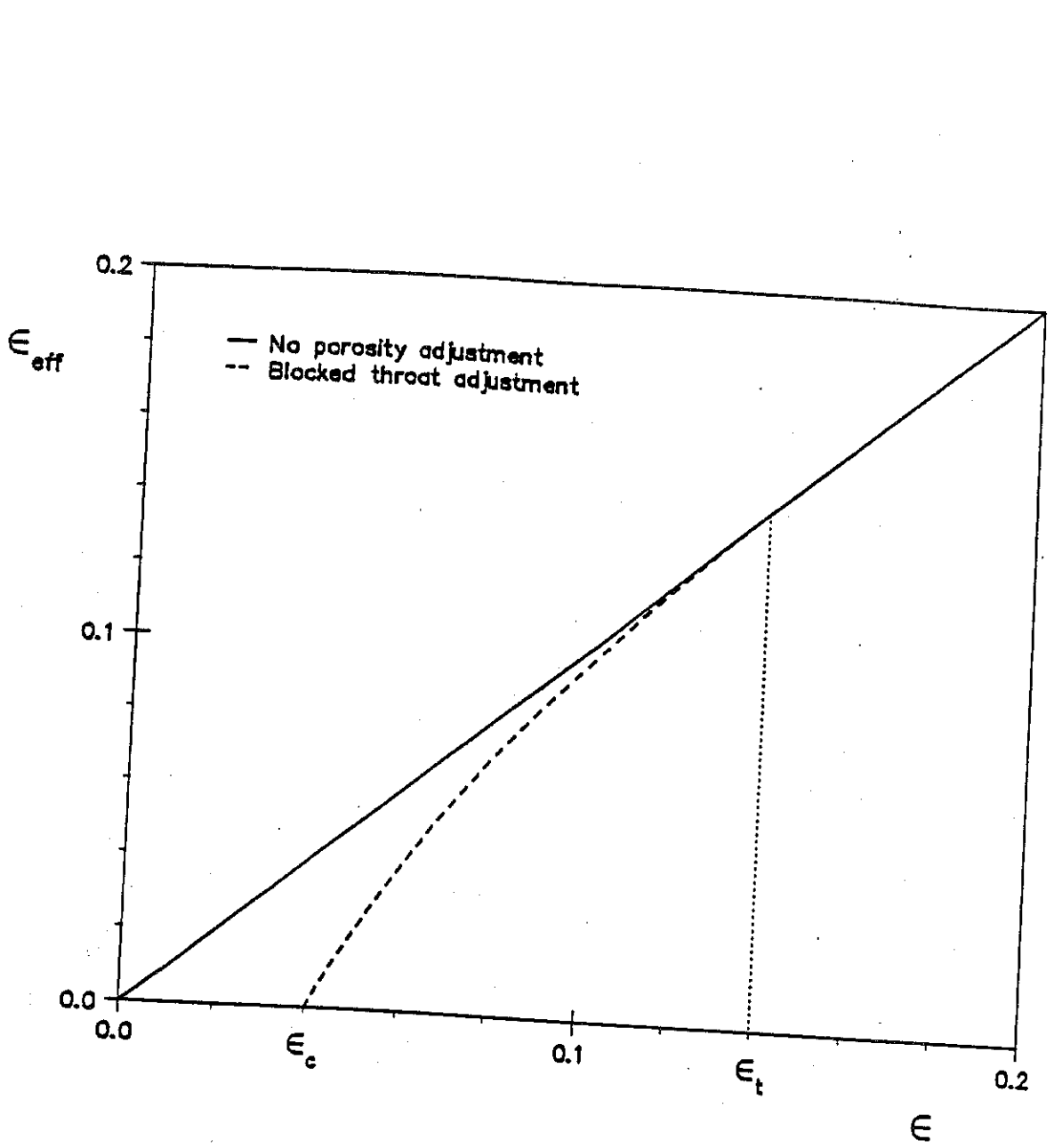

Figure 14: Definition of effective porosity.

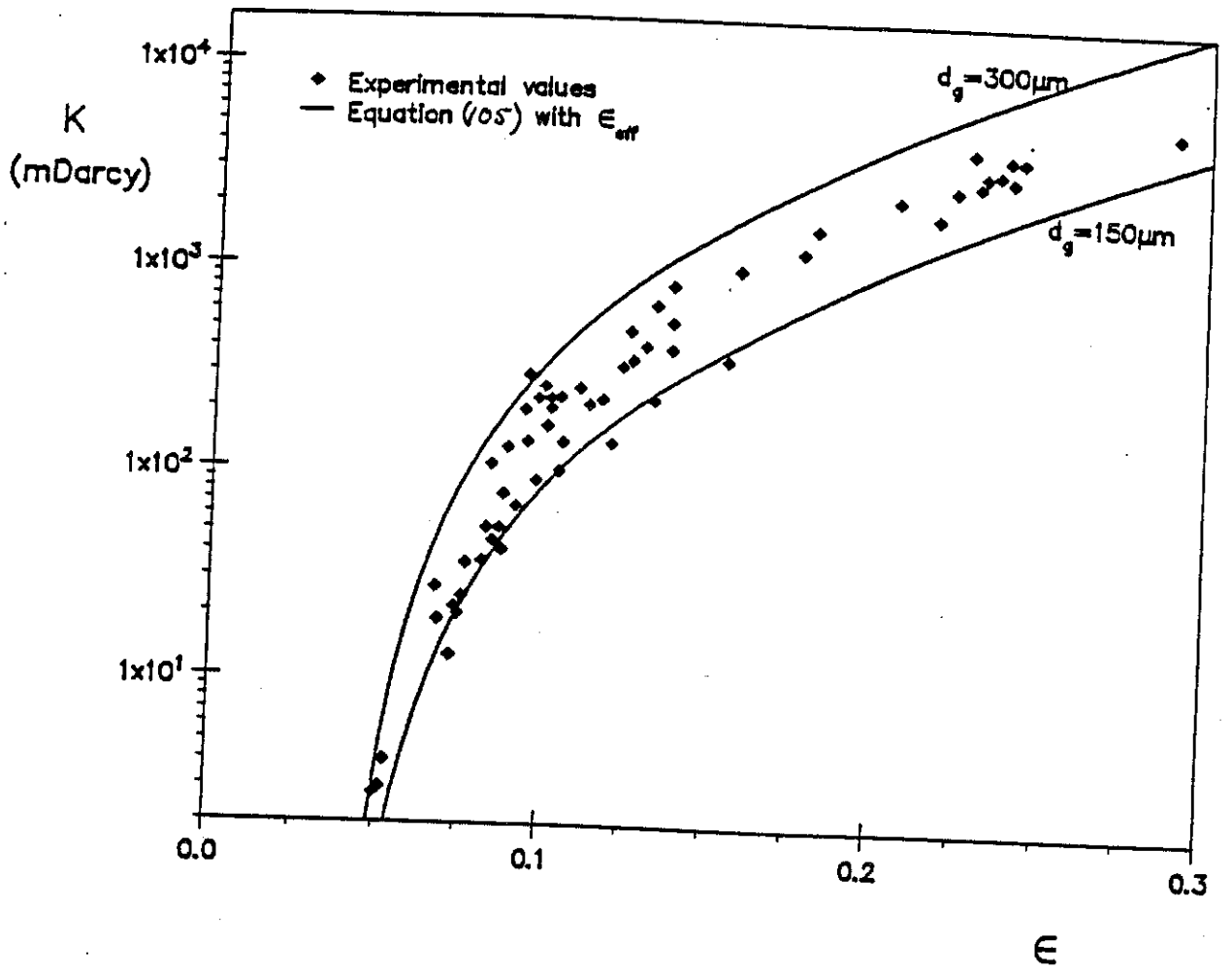

Figure 15: Final results for Fontainebleau sandstone.